

Genetic paths to evolutionary rescue and the distribution of fitness effects along them

Matthew M Osmond^{*,1}, Sarah P Otto^{*} and Guillaume Martin[†]

^{*}Biodiversity Centre & Department of Zoology, University of British Columbia, [†]Institut des Sciences de l'Evolution de Montpellier, Université Montpellier II

ABSTRACT

The past century has seen substantial theoretical and empirical progress on the genetic basis of adaptation. Over this same period a pressing need to prevent the evolution of drug resistance has uncovered much about the potential genetic basis of persistence in declining populations. However, we have little theory to predict and generalize how persistence – by sufficiently rapid adaptation – might be realized in this explicitly demographic scenario. Here we use Fisher's geometric model with absolute fitness to begin a line of theoretical inquiry into the genetic basis of evolutionary rescue, focusing here on asexual populations that adapt through *de novo* mutations. We show how the dominant genetic path to rescue switches from a single mutation to multiple as mutation rates and the severity of the environmental change increase. In multi-step rescue, intermediate genotypes that themselves go extinct provide a 'springboard' to rescue genotypes. Comparing to a scenario where persistence is assured, our approach allows us to quantify how a race between evolution and extinction leads to a genetic basis of adaptation that is composed of fewer loci of larger effect. We hope this work brings awareness to the impact of demography on the genetic basis of adaptation.

KEYWORDS Antimicrobial drug resistance; Evolutionary escape; Fisher's geometric model; Genetic basis of adaptation; Mathematical theory

Our understanding of the genetic basis of adaptation is rapidly improving due to the now widespread use of genomic sequencing (see examples in Bell 2009; Stapley *et al.* 2010; Dettman *et al.* 2012; Schlötterer *et al.* 2015). A recurrent observation, especially in experimental evolution with asexual microbes, is that the more novel the environment and the stronger the selection pressure, the more likely it is that adaptation primarily proceeds by fewer mutations of larger effect (i.e., that adaptation is oligogenic *sensu* Bell 2009). An extreme case is the evolution of drug resistance, which is often achieved by just one or two mutations (e.g., Bataillon *et al.* 2011; Pennings *et al.* 2014).

However, drugs, and other sufficiently novel environments, will often induce not only strong selection but also population decline. Such declines hinder both the production and maintenance of adaptive genetic variation (Otto and Whitlock 1997), thus impeding evolution and threatening extinction. Drug resistance evolution is a particular instance of the more general phenomenon of evolutionary rescue (Gomulkiewicz and Holt

1995; Bell 2017), where persistence requires sufficiently fast adaptive evolution.

Most theory on the genetics of adaptation (reviewed in Orr 2005) assumes constant population size and therefore does not capture the characteristic 'race' between adaptation and extinction that occurs during evolutionary rescue. Many models have been created to describe this race (reviewed in Alexander *et al.* 2014) but so far largely focus on two extreme genetic bases, both already introduced in Gomulkiewicz and Holt (1995): rescue is either caused by minute changes in allele frequencies across many loci in sexuals (i.e., the infinitesimal model; Fisher 1918) or by the substitution of a single large effect 'resistance' mutation (e.g., one locus, two allele models). We therefore largely lack a theoretical framework for the genetic basis of evolutionary rescue that captures the arguably more realistic situation where an intermediate number of mutations are at play (but see exceptions below). The near absence of such a framework prevents us from predicting the number of mutations that evolutionary rescue will take and the distribution of their effect sizes. The existence of a more complete framework could therefore provide valuable information for those investigating the genetic basis of drug resistance (e.g., the expected number and effect sizes of

55 mutations) and would extend our understanding of the genetic
56 basis of adaptation to cases of non-equilibrium demography (i.e.,
57 rapid evolution and "eco-evo" dynamics).

58 Despite these gaps in the theory on the genetic basis of evolu-
59 tionary rescue, there is a wealth of data. For example, the genetic
60 basis of resistance to a variety of drugs is known in many species
61 of bacteria (reviewed in MacLean *et al.* 2010), fungi (reviewed
62 in Robbins *et al.* 2017), and viruses (reviewed in Yilmaz *et al.*
63 2016). This abundance of data reflects both the applied need
64 to prevent drug resistance and the relative ease of isolating the
65 genotypes that survive (hereafter "rescue genotypes"), e.g., in a
66 Luria-Delbrück fluctuation assay (reviewed in Bataillon and
67 Bailey 2014). Assaying fitness in the environment used to isolate
68 mutants (e.g., in the drug) then provides the distribution of fit-
69 ness effects of potential rescue genotypes. Additional data on
70 the genetic basis of drug resistance arise from the construction
71 of mutant libraries (e.g., Weinreich *et al.* 2006) and the sequenc-
72 ing of natural populations (e.g., Pennings *et al.* 2014). Together,
73 the data show that resistance often appears to arise by a single
74 mutation (e.g., MacLean and Buckling 2009; Lindsey *et al.* 2013;
75 Gerstein *et al.* 2012) but not always (e.g., Bataillon *et al.* 2011;
76 Pennings *et al.* 2014; Gerstein *et al.* 2015; Williams and Pennings
77 2019). The data also indicate that the fitness effect of rescue ge-
78 notypes is more often large than small, creating a hump-shaped
79 distribution of selection coefficients (e.g., Kassen and Bataillon
80 2006; MacLean and Buckling 2009; Gerstein *et al.* 2012; Lindsey
81 *et al.* 2013; Gerstein *et al.* 2015) that is similar in shape to that
82 proposed by Kimura (1983) (see Orr 1998, for more discussion)
83 but with a lower bound that is often much greater than zero.

84 Theory on evolutionary rescue (reviewed in Alexander *et al.*
85 2014) has primarily focused on the probability of rescue rather
86 than its genetic basis. However, a few studies have varied the
87 potential genetic basis enough to make some inference about
88 how evolutionary rescue is likely to happen. For instance, in the
89 context of pathogen host-switching, Antia *et al.* (2003) numeri-
90 cally explored the probability of rescue starting from a single
91 ancestral individual when k sequential mutations are required
92 for a positive growth rate, each mutation occurring from the
93 previous genotype with the same probability and all intermedi-
94 ate genotypes being selectively neutral. The authors found that
95 rescue became less likely as the number of intermediate muta-
96 tions increased, suggesting that rescue will generally proceed by
97 the fewest possible mutations. This framework was expanded
98 greatly by Iwasa *et al.* (2004a), who allowed for arbitrary muta-
99 tional networks (i.e., different mutation rates between any two
100 genotypes) and standing genetic variation in the ancestral popu-
101 lation. Assuming the probability of mutation between any two
102 genotypes is of the same order, they showed that genetic paths
103 with fewer mutational steps contributed more to the total proba-
104 bility of rescue, again suggesting rescue will occur by the fewest
105 possible mutations. Iwasa *et al.* (2004a) also found that multiple
106 simultaneous mutations (i.e., arising in the same meiosis) can
107 contribute more to rescue than paths that gain these same muta-
108 tions sequentially (i.e., over multiple generations) when the
109 growth rates of the intermediate mutations are small enough,
110 suggesting that rare large mutations can be the most likely path
111 to rescue when the population is very maladapted or there is a
112 fitness valley separating the wildtype and rescue genotype. This
113 point was also demonstrated by Alexander and Day (2010), who
114 emphasized that multiple simultaneous mutations become the
115 dominant path to rescue in the most challenging environments.
116 As a counterpoint, Uecker and Hermisson (2016) explored a

117 greater range of fitness values in a two-locus two-allele model,
118 showing that, with standing genetic variation, rescue by sequen-
119 tial mutations at two loci (two mutational steps) can be more
120 likely than rescue by mutation at a single locus (one simulta-
121 neous mutational step), particularly when the wildtype is very
122 maladapted, where the single mutants can act as a buffer in
123 the face of environmental change. In summary, current theory
124 indicates that the genetic basis of rescue hinges on the chosen
125 set of genotypes, their fitnesses, and the mutation rates between
126 them. So far these choices have been in large part arbitrary or
127 chosen for mathematical convenience.

128 Here we follow the lead of Anciaux *et al.* (2018) in allowing
129 the genotypes that contribute to rescue, as well as their fitnesses
130 and the mutational distribution, to arise from an empirically-
131 justified fitness-landscape model (Tenailon 2014). In particular,
132 we use Fisher's geometric model to describe adaptation follow-
133 ing an abrupt environmental change that instigates population
134 decline. There are two key differences between this approach
135 and earlier models using Fisher's geometric model (e.g., Orr
136 1998): here 1) the dynamics of each genotype depends on their
137 absolute fitness (instead of only on their relative fitness) and 2)
138 multiple mutations can segregate simultaneously (instead of as-
139 suming only sequential fixation), allowing multiple mutations to
140 fix – and in our case, rescue the population – together as a single
141 haplotype (i.e., stochastic tunnelling, Iwasa *et al.* 2004b). In this
142 non-equilibrium scenario, variation in absolute fitness, which
143 allows population size to vary, can create feedbacks between
144 demography and evolution, which could strongly impact the
145 genetic basis of adaptation relative to the constant population
146 size case. In contrast to Anciaux *et al.* (2018), our focus here is
147 on the genetic basis of evolutionary rescue and we also explore
148 the possibility of rescue by mutant haplotypes containing more
149 than one mutation. In particular, we ask: (1) How many muta-
150 tional steps is evolutionary rescue likely to take? and (2) What
151 is the expected distribution of fitness effects of the surviving
152 genotypes and their component mutations?

153 We first introduce the modelling framework before summa-
154 rizing our main results. We then present the mathematical anal-
155 yses we have used to understand these results and end with a
156 discussion of our key findings.

157 Data availability

158 Code used to derive analytical and numerical results and pro-
159 duce figures (referred to here as File S1; *Mathematica*, ver-
160 sion 9.0; Wolfram Research Inc. 2012) and code used to create
161 individual-based simulation data (Python, version 3.5; Python
162 Software Foundation), as well as simulation data and freely
163 accessible versions of File S1 (CDF and PDF), are available at
164 <https://github.com/mmosmond/GeneticBasisOfRescue>.

165 Model

166 Fisher's geometric model

167 We map genotype to phenotype to fitness using Fisher's geo-
168 metric model, originally introduced by Fisher (1930, p. 38-41)
169 and reviewed by Tenailon (2014). In this model each geno-
170 type is characterized by a point in n -dimensional phenotypic
171 space, \vec{z} . We ignore environmental effects, and thus the phe-
172 notype is the breeding value. At any given time there is a
173 phenotype, \vec{o} , that has maximum fitness and fitness declines
174 monotonically as phenotypes depart from \vec{o} . We assume that
175 n phenotypic axes can be chosen and scaled such that fitness

is described by a multivariate Gaussian function with variance 1 in each dimension, no covariance, and height W_{max} (which can always be done when considering genotypes close enough to a non-degenerate optimum; [Martin 2014](#)). Thus the fitness of phenotype \vec{z} is $W(\vec{z}) = W_{max} \exp(-\|\vec{z} - \vec{o}\|^2/2)$, where $\|\vec{z} - \vec{o}\| = \sqrt{\sum_{i=1}^n (z_i - o_i)^2}$ is the Euclidean distance of \vec{z} from the optimum, \vec{o} . Here we are interested in absolute fitness; we take $\ln[W(\vec{z})] = m(\vec{z}) = m_{max} - \|\vec{z} - \vec{o}\|^2/2$ to be the continuous-time growth rate (m is for Malthusian fitness) of phenotype \vec{z} . We ignore density- and frequency-dependence in $m(\vec{z})$ for simplicity. The fitness effect, i.e., selection coefficient, of phenotype z' relative to z in a continuous-time model is exactly $s = \log[W(z')/W(z)] = m(z') - m(z)$ ([Martin and Lenormand 2015](#)). This is approximately equal to the selection coefficient in discrete time ($W(z')/W(z) - 1$) when selection is weak ($W(z') - W(z) \ll 1$).

To make analytical progress we use the isotropic version of Fisher's geometric model, where mutations (in addition to selection) are assumed to be uncorrelated across the scaled traits. Universal pleiotropy is also assumed, so that each mutation affects all scaled phenotypes. In particular we use the "classic" form of Fisher's geometric model ([Harmand et al. 2017](#)), where the probability density function of a mutant phenotype is multivariate normal, centred on the current phenotype, with variance λ in each dimension and no covariance. Using a probability density function of mutant phenotypes implies a continuum-of-alleles ([Kimura 1965](#)), i.e., phenotype is continuous and each mutation is unique. Mutations are assumed to be additive in phenotype, which induces epistasis in fitness (as well as dominance under diploid selection), as fitness is a non-linear function of phenotype. We assume asexual reproduction, i.e., no recombination, which is appropriate for many cases of antimicrobial drug resistance and experimental evolution, while recognizing the value of expanding this work to sexual populations.

An obvious and important extension would be to relax the simplifying assumptions of isotropy and universal pleiotropy, which we leave for future work. Note that mild anisotropy yields the same bulk distribution of fitness effects as an isotropic model with fewer dimensions ([Martin and Lenormand 2006](#)), but this does not extend to the tails of the distribution. Therefore, whether anisotropy can be reduced to isotropy with fewer dimensions in the case of evolutionary rescue, where the tails are essential, is unknown. In the [Discussion](#) we briefly explore the effects of non-Gaussian distributions of mutant phenotypes.

Given this phenotype-to-fitness mapping and phenotypic distribution of new mutations, the distribution of fitness effects (and therefore growth rates) of new mutations can be derived exactly. Let m be the growth rate of some particular focal genotype and m' the growth rate of a mutant immediately derived from it. Then let $s_o = m_{max} - m$ be the selective effect of a mutant with the optimum genotype and $s = m' - m$ the selective effect of the mutant with growth rate m' . The probability density function of the selective effects of new mutations, s , is then given by equation 3 in [Martin and Lenormand \(2015\)](#). Converting fitness effects to growth rate ($m' = s + m$), the probability density function for mutant growth rate m' from an ancestor with growth rate m is (cf. equation 2 in [Anciaux et al. 2018](#))

$$f(m'|m) = \frac{2}{\lambda} f_{\chi_n^2} \left(\frac{2(m_{max} - m')}{\lambda}, \frac{2(m_{max} - m)}{\lambda} \right), \quad (1)$$

where $f_{\chi_n^2}(x, c)$ is the probability density function over positive

real numbers x of $\chi_n^2(c)$, a non-central chi-square deviate with n degrees of freedom and noncentrality $c > 0$ (equation 26.4.25 in [Abramowitz and Stegun 1972](#)).

Lifecycle

We are envisioning a scenario where N_0 wildtype individuals, each of which have phenotype \vec{z}_0 , experience an environmental change, causing population decline, $m_0 \equiv m(\vec{z}_0) < 0$. Each generation, an individual with phenotype \vec{z} produces a Poisson number of offspring, with mean $\ln[m(\vec{z})]$, and dies. This process implicitly assumes no interaction between individuals, i.e., a branching process with density- and frequency-independent growth and fitness and no clonal interference. Each offspring mutates with probability U (we ignore the possibility of multiple simultaneous mutations within a single genome), and mutations are distributed as described above (see [Fisher's geometric model](#)).

Simulation procedure

We ran individual-based simulations of the above process to compare with our numeric and analytic results. Populations were considered rescued when there were ≥ 1000 individuals (Figures 1-3) or ≥ 100 individuals (Figures 6-7, S1, and S3) with positive growth rates (all other replicates went extinct). The most common genotype at the time of rescue was considered the rescue genotype, and the number of mutational steps to rescue was set as the number of mutations in that genotype.

Probability of rescue

Let p_0 be the probability that a given wildtype individual is "successful", i.e., has descendants that rescue the population. The probability of rescue is then one minus the probability that none of the initial wildtype individuals are successful,

$$P = 1 - (1 - p_0)^{N_0} \approx 1 - \exp(-N_0 p_0), \quad (2)$$

where the approximation assumes small p_0 and large N_0 . What remains is to find p_0 .

Summary of Results

We start with a heuristic explanation of our main results before turning to more detailed derivations in the next section.

Rescue by multiple mutations

A characteristic pattern of evolutionary rescue is a "U"-shaped population size trajectory (e.g., [Orr and Unckless 2014](#)). This is the result of an exponentially-declining wildtype genotype being replaced by an exponentially-increasing mutant genotype. On a log scale this population size trajectory becomes "V"-shaped (we denote it a 'V-shaped log-trajectory'). On this scale, the population declines at a constant rate (producing a line with slope $m_0 < 0$) until the growing mutant subpopulation becomes relatively common, at which point the population begins growing at a constant rate (a line with slope $m_1 > 0$). This characteristic V-shaped log-trajectory is observed in many of our simulations where evolutionary rescue occurs (Figure 1A). Alternatively, when the wildtype declines faster and the mutation rate is larger we sometimes see 'U-shaped log-trajectories' (e.g., the red and blue replicates in Figure 2A). Here there are three phases instead of two; the initial rate of decline (a line with slope $m_0 < 0$) is first reduced (transitioning to a line with slope $m_1 < 0$) before the population begins growing (a line with slope $m_2 > 0$).

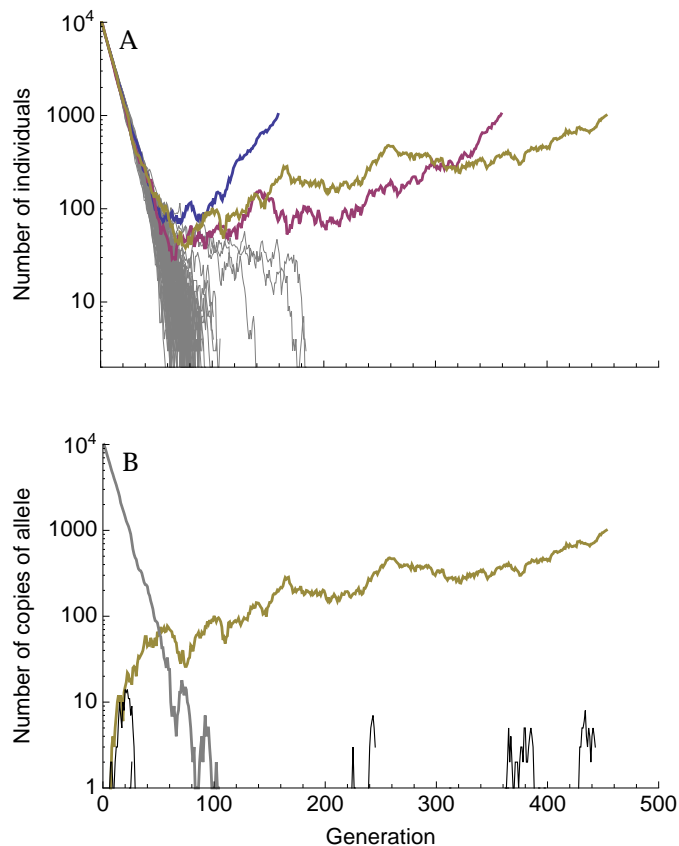


Figure 1 Typical dynamics with a relatively slow wildtype decline and a small mutation rate ($m_0 = -0.1$, $U = 10^{-4}$). (A) Population size trajectories on a log scale. Each line is a unique replicate simulation (100 replicates). Replicates that went extinct are grey, replicates that were rescued are in colour (and are roughly V-shaped). (B) The number of individuals with a given derived allele, again on a log scale, for the yellow replicate in A. The number of individuals without any derived alleles (wildtypes) is shown in grey, the rescue mutation is shown in yellow, and all other mutations are shown in black. Other parameters: $n = 4$, $\lambda = 0.005$, $m_{max} = 0.5$.

As expected, V-shaped log-trajectories are the result of a single mutation creating a genotype with a positive growth rate that escapes loss when rare and rescues the population (Figure 1B), i.e., 1-step rescue. U-shaped log-trajectories, on the other hand, occur when a single mutation creates a genotype with a negative (or potentially very small positive) growth rate, itself doomed to extinction, which out-persists the wildtype and gives rise to a double mutant genotype that rescues the population (Figure 2B), i.e., 2-step rescue. These two types of rescue comprise the overwhelming majority of rescue events observed in our simulations, across a wide range of wildtype decline rates (e.g., Figure 3).

In the text, we focus on low to moderate mutation rates affecting growth rate. With sufficiently high mutation rates rescue by 3 or more mutations comes to dominate (Figure S1). It has recently been suggested that when the mutation rate, U , is substantially less than a critical value, $U_C = \lambda n^2/4$, we are in a “strong selection, weak mutation” regime where selection is strong enough relative to mutation that essentially all mutations arise on a wildtype background (Martin and Roques 2016), con-

sistent with the House of Cards approximation (Turelli 1984, 1985). Thus in this regime rescue tends to occur by a single mutation of large effect (Anciaux et al. 2018). In the other extreme, when $U \gg U_C$, we are in a “weak selection, strong mutation” regime where selection is weak enough relative to mutation that many cosegregating mutations are present within each genome, creating a multivariate normal phenotypic distribution (Martin and Roques 2016), consistent with the Gaussian approximation (Kimura 1965; Lande 1980). Thus in this regime rescue tends to occur by many mutations of small effect (Anciaux et al. 2019). As shown in Figure 3 (where $U = U_C/10$) and Figure S1 (where $U_C = 0.02$), rescue by a small number of mutations (but more than one) can become commonplace in the transition zone (where U is neither much smaller or much larger than U_C), where there are often a considerable number of cosegregating mutations (e.g., Figure 2B, where $U = U_C/2$).

The probability of k -step rescue

Approximations for the probability of 1-step rescue under the strong selection, weak mutation regime were derived by Anciaux et al. (2018). Here we extend this study by exploring the contribution of k -step rescue, deriving approximations for the probability of such events, as well as dissecting the genetic basis of both 1- and 2-step rescue in terms of the distribution of fitness effects of rescue genotypes and their component mutations.

Although requiring a sufficiently beneficial mutation to arise on a rare mutant genotype doomed to extinction, multi-step evolutionary rescue can be the dominant form of rescue when the wildtype is sufficiently maladapted (Figures 3 and S1). Indeed, on this fitness landscape, the probability of producing a rescue genotype in one mutational step mutant drops very sharply with maladaptation (Anciaux et al. 2018); the probability of multi-step rescue declines more slowly as mutants with intermediate growth rates can be a “springboard” – albeit not always a very bouncy one – from which rescue mutants are produced. These intermediates contribute more as mutation rates and the decline rate of the wildtype increase (Figures 3 and S1), the former because double mutants become more likely and the latter because the springboard becomes more necessary. With a large enough number of wildtype individuals or a high enough mutation rate (Figure S1), multi-step rescue can not only be more likely than 1-step, but also very likely in an absolute sense.

Classifying 2-step rescue regimes

2-step rescue can occur through first-step mutants with a wide range of growth rates. As shown below (see Approximating the probability of 2-step rescue), these first-step mutants can be divided into three regimes: “sufficiently subcritical”, “sufficiently critical”, and “sufficiently supercritical” (we will often drop “sufficiently” for brevity; Figure 4). Sufficiently critical first-step mutants are defined by having growth rates close enough to zero that the most likely way for such a mutation to lead to 2-step rescue is for it to persist for such an unusually long period of time, and accordingly grow to such an unusually large subpopulation size, that it will almost certainly produce successful double mutants. Sufficiently subcritical first-step mutants are then defined by having growth rates that are negative enough to almost certainly prevent such long persistence times. Instead, these mutations tend to persist for an expected number of generations, proportional to the inverse of their growth rate ($1/|m|$), while maintaining relatively small subpopulation sizes (on the order of one individual per generation). Mutations conferring

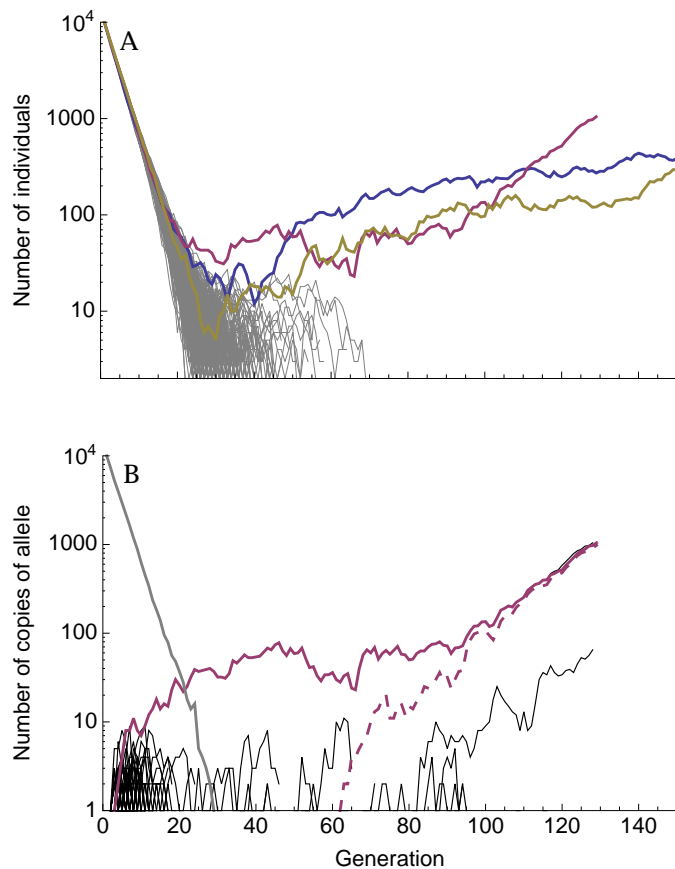


Figure 2 Typical dynamics with a relatively fast wildtype decline and a large mutation rate ($m_0 = -0.3$, $U = 10^{-2}$). **(A)** Population size trajectories on a log scale. Each line is a unique replicate simulation (500 replicates). Replicates that went extinct are grey, replicates that were rescued are in colour. Note that the blue and red replicates are cases of 2-step rescue (and roughly U-shaped), while the yellow replicate is 1-step rescue (and therefore V-shaped). **(B)** The number of individuals with a given derived allele, again on a log scale, for the red replicate in **A**. The number of individuals without any derived alleles (wildtypes) is shown in grey, the rescue mutations are shown in red, and all other mutations in black. Here a single mutant with growth rate less than zero arises early and outlives the wildtype (solid red). A second mutation then arises on that background (dashed red), making a double mutant with a growth rate greater than zero that rescues the population. Other parameters: $n = 4$, $\lambda = 0.005$, $m_{max} = 0.5$.

a positive growth rate can also go extinct, and thus can also act as springboards to rescue. Conditioned on extinction, supercritical mutations behave like subcritical mutations with a growth rate of the same absolute value (Maruyama and Kimura 1974). Sufficiently supercritical first-step mutants are therefore defined analogously to subcritical first-step mutants, having positive (rather than negative) growth rates that are large enough to prevent sufficiently long persistence times once conditioned on extinction. Despite having similar extinction trajectories as subcritical mutations, ‘doomed’ supercritical mutations arise less frequently by mutation from the wildtype but mutate to rescue genotypes at a higher rate. Overall, they too can contribute substantially to rescue. Note that supercritical 2-step rescue is

not 1-step rescue with subsequent adaptation as we condition on the first-step mutation going extinct in the absence of the second mutation. However, empirically it will be impossible to tell if the first-step mutation was indeed doomed to extinction if it is found to have a positive growth rate in the selective environment.

The relative contribution of each regime changes with both the initial degree of maladaptation and the mutation rate (Figures 5 and S2). When the wildtype is very maladapted (relative to mutational variance), most 2-step rescue events occur through subcritical first-step mutants (Figure 5A), which arise at a higher rate than critical or supercritical mutants and yet persist longer than the wildtype. When the wildtype is less maladapted, however, critical and supercritical mutations become increasingly likely to arise and contribute to 2-step rescue, both due to their closer proximity to the wildtype in phenotypic space as well as the slower decline of the wildtype increasing the cumulative number of mutations that occur. The mutation rate also plays an interesting role in determining the relative contributions of each regime (Figures 5B and S2). When mutations are rare, only first-step mutations that are very nearly neutral ($m \sim 0$) will persist long enough to give rise to a 2-step rescue mutation. As the mutation rate increases, however, the range of first-step mutant growth rates that can persist long enough to lead to 2-step rescue widens because fewer individuals carrying the first-step mutation are needed before a successful double mutant arises.

The distribution of fitness effects among rescue mutations

Mutants causing 1-step rescue have growth rates that cluster around small positive values ($m \gtrsim 0$; blue curves in Figure 6). Consequently, the distribution of fitness effects (DFE) among these rescue mutants is shifted to the right relative to mutations that establish in a population of constant size (compare solid blue and gray curves in Figure 6), with a DFE beginning at $s = m - m_0 \geq -m_0 > 0$ rather than $s = 0$ (Kimura 1983). As a result of this increased threshold, the 1-step rescue DFE has a smaller variance than both the DFE of random mutations and the DFE of mutations that establish in a constant population (compare blue and gray curves in Figure 6). Further, while the variance in the DFE of random mutations and of those that establish in a population of constant size increases slightly with initial maladaptation (due to the curvature of the phenotype-to-fitness function), the variance in the 1-step rescue DFE decreases substantially (compare panels in Figure 6), as rescue becomes restricted to a rapidly decreasing proportion of the available mutants.

The DFE of genotypes that cause 2-step rescue (the combined effect of two mutations) is also clustered at small positive growth rates, but it has a variance that is less affected by the rate of wildtype decline (red curves in Figure 6). This is because double mutant rescue genotypes are created via first-step mutant genotypes that have larger growth rates than the wildtype (i.e., are closer to the optimum), allowing them to create double mutants with a larger range of positive growth rates.

Finally, we can also look at the distribution of growth rates among first-step mutations that lead to 2-step rescue, i.e., ‘springboard mutants’ (Figures 7 and S2). Here there are two main factors to consider: 1) the probability that a mutation with a given growth rate arises on the wildtype background but does not by itself rescue the population and 2) the probability that such a mutation persists long enough for a sufficiently beneficial second mutation to arise on that same background and together

442 rescue the population. Subcritical mutations conferring growth
 443 rates closer to zero persist longer but are less likely to arise from
 444 the wildtype, creating a trade-off between mutational input and
 445 the probability of rescue that can lead to a wide distribution
 446 of contributing subcritical growth rates (blue shading in Fig-
 447 ure 7). In contrast, supercritical mutations with growth rates
 448 nearer to zero are more likely arise by mutation, to go extinct in
 449 the absence of further mutation, and to persist for longer once
 450 conditioned on extinction, together creating a relatively narrow
 451 distribution of contributing supercritical growth rates (yellow
 452 shading in Figure 7). As explained above, increasing the rate of
 453 wildtype decline (or decreasing the rate of mutation) increases
 454 the contribution of subcritical first-step mutants and the impor-
 455 tance of mutational input, lowering the mode and increasing the
 456 variance of the first-step DFE (compare panels in Figure 7).

457 Note that, given 2-step rescue, the growth rate of both the
 458 first-step and second-step mutation may be negative when con-
 459 sidered by themselves in the wildtype background. This poten-
 460 tially obscures empirical detection of the individual mutations
 461 involved in evolutionary rescue.

462 Mathematical Analysis

463 The probability of k -step rescue

464 Generic expressions for the probability of 1- and 2-step rescue
 465 were given by [Martin et al. \(2013\)](#), using a diffusion approxima-
 466 tion of the underlying demographics. The key result that we
 467 will use is the probability that a single copy of a genotype with
 468 growth rate m , itself fated for extinction but which produces
 469 rescue mutants at rate $\Lambda(m)$, rescues the population (equation
 470 S1.5 in [Martin et al. 2013](#)). With our lifecycle this is (c.f., equation
 471 A.3 in [Iwasa et al. 2004a](#))

$$p(m, \Lambda(m)) = 1 - \exp \left[|m| \left(1 - \sqrt{1 + \frac{2\Lambda(m)}{m^2}} \right) \right]. \quad (3)$$

472 We can therefore use $p_0 = p(m_0, \Lambda(m_0))$ as the probability that a
 473 wildtype individual has descendants that rescue the population
 474 and what remains in calculating the total probability of rescue
 475 (Equation 2) is $\Lambda(m_0)$. We break this down by letting $\Lambda_i(m)$ be
 476 the rate at which rescue genotypes with i mutations are created;
 477 the total probability of rescue is then given by Equation 2 with
 478 $p_0 = p(m_0, \sum_{i=1}^{\infty} \Lambda_i(m_0))$.

479 In 1-step rescue, $\Lambda_1(m_0)$ is just the rate of production of res-
 480 cue mutants directly from a wildtype genotype. This is the
 481 probability that a wildtype gives rise to a mutant with growth
 482 rate m (given by $Uf(m|m_0)$) times the probability that a geno-
 483 type with growth rate m establishes. Again approximating our
 484 discrete time process with a diffusion process, the probability
 485 that a lineage with growth rate $m \ll 1$ establishes, ignoring
 486 further mutation, is (e.g., [Martin et al. 2013](#))

$$p_{est}(m) \approx \begin{cases} 0 & m \leq 0 \\ 1 - \exp(-2m) & m > 0 \end{cases}. \quad (4)$$

487 This reduces to the $2(s + m_0)$ result in [Otto and Whitlock \(1997\)](#)
 488 when $m = s + m_0$ is small, which further reduces to $2s$ in
 489 a population of constant size, where $m_0 = 0$ ([Haldane 1927](#)). Using
 490 this, the rate of 1-step rescue is

$$\Lambda_1(m_0) = U \int_0^{m_{max}} f(m|m_0) p_{est}(m) dm. \quad (5)$$

Symbol	Meaning
n	number of (scaled) phenotypic dimensions
λ	variance in mutant phenotypes along each di- dimension
m_{max}	maximum growth rate
$f(m' m)$	distribution of growth rates among mutants from a genotype with growth rate m (eq. 1)
U	per genome mutation probability
N_0	initial number of wildtype individuals
m_0	wildtype growth rate
p_0	probability a wildtype individual has descen- dants that rescue the population
P	probability of rescue (eq. 2)
$p(m, \Lambda(m))$	probability a genotype with growth rate m , it- self fated for extinction, has descendants that rescue the population (eq. 3)
$p_{est}(m)$	probability a genotype with growth rate m es- tablishes, i.e., rescues the population (eq. 4)
$\Lambda(m)$	probability that an individual with growth rate m produces a mutant that has descendants that rescue the population
$\Lambda_i(m)$	probability that an individual with growth rate m produces a mutant that has descendants with $i - 1$ additional mutations that rescue the pop- ulation
$\Lambda_2^i(m)$	probability that an individual with growth rate m produces sufficiently subcritical ($i = "-"$), critical ($i = 0$), or supercritical ($i = "+"$) first- step mutants that eventually lead to 2-step res- cue (eq. 8)
ψ	$2(1 - \sqrt{1 - m/m_{max}})$
ψ_0	$2(1 - \sqrt{1 - m_0/m_{max}})$
ρ_{max}	m_{max}/λ
α	$\rho_{max}\psi_0^2/4$

Table 1 Frequently used notation.

491 Taking the first order approximation of $p(m_0, \Lambda_1(m_0))$ with
 492 $\Lambda_1(m_0)/m_0^2$ small gives the probability of 1-step rescue (equa-
 493 tion 5 of [Anciaux et al. 2018](#)), which effectively assumes deter-
 494 ministic wildtype decline. For completeness we rederive their
 495 closed-form approximation in File S1 (and give the results in the
 496 Appendix, see [Approximating the probability of 1-step rescue](#)).

497 The probability of 2-step rescue is only slightly more compli-
 498 cated. Here $\Lambda_2(m_0)$ is the probability that a mutation arising on
 499 the wildtype background creates a genotype that is also fated
 500 for extinction but persists long enough for a second mutation
 501 to arise on this mutant background, creating a double mutant
 502 genotype that rescues the population. We therefore have

$$\Lambda_2(m_0) = U \int_{-\infty}^{m_{max}} f(m|m_0) [1 - p_{est}(m)] p(m, \Lambda_1(m)) dm. \quad (6)$$

503 Following this logic, we can retrieve the probability of k -step
504 rescue, for arbitrary $k \geq 2$, using the recursion

$$\Lambda_k(m_0) = U \int_{-\infty}^{m_{max}} f(m|m_0) [1 - p_{est}(m)] p(m, \Lambda_{k-1}(m)) dm, \quad (7)$$

505 with the initial condition given by Equation 5.

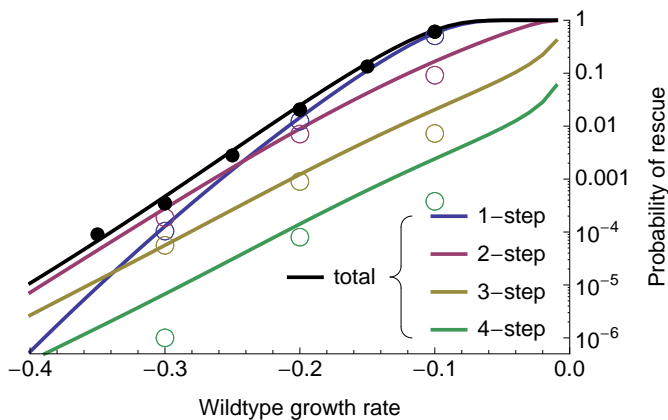


Figure 3 The probability of evolutionary rescue as a function of initial maladaptation. Shown are the probabilities of 1-, 2-, 3-, and 4-step rescue (using Equations 2-7), as well as the probability of rescue by up to 4 mutational steps ("total", using $\Lambda(m_0) = \sum_{i=1}^4 \Lambda_i(m_0)$). Circles are individual-based simulation results (ranging from 10^5 to 10^6 replicates per wildtype growth rate). Open circles denote the fraction of simulations where the rescue genotype (see Simulation procedure) had a given number of mutations and closed circles are the sum of these fractions. Parameters: $N_0 = 10^4$, $U = 2 \times 10^{-3}$, $n = 4$, $\lambda = 0.005$, $m_{max} = 0.5$.

506 Approximating the probability of 2-step rescue

507 The probability of 2-step rescue is given by Equation 2 with
508 $p_0 = p(m_0, \Lambda_2(m_0))$ (Equations 3-6). We next develop some
509 intuition by approximating this for different classes of single
510 mutants.

511 First, note that when the growth rate of a first-step mutation
512 is close enough to zero such that $m^2 \ll \Lambda_1(m)$, we can ap-
513 proximate the probability that such a genotype leads to rescue
514 before itself going extinct, $p(m, \Lambda_1(m))$, using a Taylor series,
515 as $\sqrt{2\Lambda_1(m)}$ (c.f. equation A.4b in Iwasa et al. 2004a, see also
516 File S1). We can also derive this result heuristically by consid-
517 ering the probability that a lineage will persist long enough
518 that it will incur a secondary rescue mutation. As shown in the
519 Appendix (see Mutant lineage dynamics), while $t < 1/|m|$ a
520 mutant lineage with growth rate m that is destined for extinction
521 persists for t generations with probability $\sim 2/t$ (Equation 21)
522 and in generation t since it has arisen has $\sim t/2$ individuals
523 (Equation 22). Thus, while $T < 1/|m|$ a mutant lineage that
524 persists for T generations will have produced a cumulative num-
525 ber $\sim T^2/4$ individuals. Such lineages will then lead to 2-step
526 rescue with probability $\sim \Lambda_1(m)T^2/4$ until this approaches 1,

527 near $T = 2/\sqrt{\Lambda_1(m)}$. Since the probability of rescue increases
528 like T^2 while the probability of persisting to time T declines only
529 like $1/T$, most rescue events will be the result of rare long-lived
530 single mutant genotypes. Considering only the most long-lived
531 genotypes, the probability that a first-step mutation leads to
532 rescue is then the probability that it survives long enough to
533 almost surely rescue, i.e., for $T \sim 2/\sqrt{\Lambda_1(m)}$ generations. Since
534 the probability of such a long-lived lineage is $2/T \sim \sqrt{\Lambda_1(m)}$,
535 this heuristic result agrees with our Taylor series approximation
536 of Equation 5. Thus, for first-step mutants with growth rates
537 satisfying $2/\sqrt{\Lambda_1(m)} < 1/|m|$, implying $m^2 \ll \Lambda_1(m)$, which
538 occur with probability $\sim \sqrt{\Lambda_1(m)}$, persistence is long enough
539 to almost certainly ensure rescue. This same reasoning has been
540 used to explain why the probability that a neutral mutation seg-
541 regates long enough to produce a second mutation is $\sim \sqrt{U}$ in a
542 population of constant size (Weissman et al. 2009).

543 At the other extreme, when the growth rate of a first-step
544 mutation is far enough from zero such that $m^2 \gg \Lambda_1(m)$, we
545 can approximate $p(m, \Lambda_1(m))$, again using a Taylor series, with
546 $\Lambda_1(m)/|m|$ (c.f. equation A.4c in Iwasa et al. 2004a, see also File
547 S1). Conditioned on extinction such genotypes cannot persist
548 long enough to almost surely lead to 2-step rescue. Instead, we
549 expect such mutations to persist for at most $\sim 1/|m|$ genera-
550 tions (Equation 21) with a lineage size of ~ 1 individual per
551 generation (Equation 22), and thus produce a cumulative total
552 of $\sim 1/|m|$ individuals. The probability of 2-step rescue from
553 such a first-step mutation is therefore $\Lambda_1(m)/|m|$, and again this
554 heuristic argument matches our Taylor series approach. This
555 same reasoning explains why a rare mutant genotype with selec-
556 tion coefficient $|s| \gg 0$ in a constant population size model is
557 expected to have a cumulative number of $\sim 1/|s|$ descendants,
558 given it eventually goes extinct (Weissman et al. 2009).

559 The transitions between these two regimes occur when
560 $\Lambda_1(m)/|m| = \sqrt{2\Lambda_1(m)}$, i.e., when $|m| = \sqrt{\Lambda_1(m)}/2$. We
561 call single mutants with growth rates $m < -\sqrt{\Lambda_1(m)}/2$ "suf-
562 ficiently subcritical", those with $|m| < \sqrt{\Lambda_1(m)}/2$ "sufficiently
563 critical", and those with $m > \sqrt{\Lambda_1(m)}/2$ "sufficiently super-
564 critical". Given that U and thus $\Lambda_1(m)$ will generally be small, m
565 will also be small at these transition points, meaning we can
566 approximate the transition points as $m^* = \sqrt{\Lambda_1(0)}/2$ and $-m^*$.
567 We then have an approximation for the rate of 2-step rescue,

$$\begin{aligned} \Lambda_2(m_0) &= \Lambda_2^{(-)}(m_0) + \Lambda_2^{(0)}(m_0) + \Lambda_2^{(+)}(m_0) \\ \Lambda_2^{(-)}(m_0) &= U \int_{-\infty}^{-m^*} f(m|m_0) \Lambda_1(m) / |m| dm \\ \Lambda_2^{(0)}(m_0) &= U \int_{-m^*}^{m^*} f(m|m_0) [1 - p_{est}(m)] \sqrt{2\Lambda_1(m)} dm \\ \Lambda_2^{(+)}(m_0) &= U \int_{m^*}^{m_{max}} f(m|m_0) [1 - p_{est}(m)] \Lambda_1(m) / |m| dm \end{aligned} \quad (8)$$

568 where $\Lambda_2^{(i)}(m_0)$ is the rate of 2-step rescue through sufficiently
569 subcritical first-step mutants ($i = "-"$), sufficiently critical
570 first-step mutants ($i = 0$), or sufficiently supercritical first-step
571 mutants ($i = "+"$). A schematic depicting the 1- and 2-step
572 genetic paths to rescue is given in Figure 4.

573 **Closed-form approximation for critical 2-step rescue** When U
574 is small m^* is also small, allowing us to use $m = 0$ within the
575 integrand of $\Lambda_2^{(0)}(m_0)$, which spans a range, $[-m^*, m^*]$, of width
576 $2m^* \approx \sqrt{2\Lambda_1(0)}$, giving

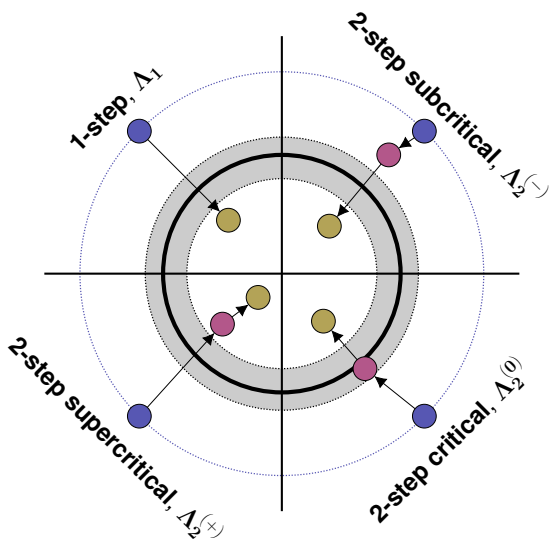


Figure 4 1- and 2-step genetic paths to evolutionary rescue. Here we show an $n = 2$ dimensional phenotypic landscape. Continuous-time (Malthusian) growth rate (m) declines quadratically from the centre, becoming negative outside the thick black line. The grey zone indicates where growth rates are “sufficiently critical” (see text for details). Blue circles show wildtype phenotypes, red circles show intermediate first-step mutations, and yellow circles show the phenotypes of rescue genotypes.

$$\begin{aligned}\Lambda_2^{(0)}(m_0) &\approx Uf(0|m_0)\sqrt{2\Lambda_1(0)}2m^* \\ &= 2Uf(0|m_0)\Lambda_1(0).\end{aligned}\quad (9)$$

We can then approximate $\Lambda_1(m)$ with $\tilde{\Lambda}_1(m)$ (Equation 19) and take $m \rightarrow 0$ (Equation 20), giving a closed form approximation for the rate of 2-step rescue through critical single mutants in Fisher’s geometric model,

$$\Lambda_2^{(0)}(m_0) \approx 4U^2f(0|m_0)\sqrt{m_{max}\lambda/\pi}.\quad (10)$$

This well approximates numerical integration of $\Lambda_2^{(0)}(m_0)$ (Equation 8; see Figure 5 and File S1). In general, it will perform better when the critical zone, and thus $U\sqrt{m_{max}\lambda}$, becomes smaller.

To get a better understanding of how the rate of 2-step critical rescue depends on the underlying parameters of Fisher’s geometric model, we approximate $f(m|m_0)$, assuming that the distance from the wildtype to the optimal phenotype is large relative to the distribution of mutations (i.e., $\rho_{max} = m_{max}/\lambda$ is large), and convert this to a distribution over $\psi = 2(1 - \sqrt{1 - m/m_{max}})$, a convenient rescaling (for details see File S1 and Anciaux *et al.* 2018). Evaluating this at $m = 0$ gives

$$\Lambda_2^{(0)}(m_0) \approx U^2(1 - \psi_0/2)^{(1-n)/2}e^{-\alpha}\frac{2}{\pi},\quad (11)$$

where $\psi_0 = 2(1 - \sqrt{1 - m_0/m_{max}}) < 0$ and $\alpha = \rho_{max}\psi_0^2/4$.

Closed-form approximations for non-critical 2-step rescue We can also approximate $\Lambda_1(m)$ in $\Lambda_2^{(-)}(m_0)$ and $\Lambda_2^{(+)}(m_0)$ with $\tilde{\Lambda}_1(m)$ (Equation 19), leaving us with just one integral over

the growth rates of the first-step mutations. We then replace $f(m|m_0)$ with its approximate distribution over ψ as above.

In the case of subcritical rescue we can then make two contrasting approximations (see File S1 for details). First, when the ψ (and thus m) that contribute most are close enough to zero (meaning maladaptation is not too large relative to mutational variance) and we ignore mutations that are less fit than the wildtype, we find the rate of subcritical 2-step rescue is roughly

$$\Lambda_2^{(-)}(m_0) \approx U^2\frac{(1 - \psi_0/2)^{1-n}}{1 - \psi_0/4}e^{-\alpha}\frac{\log(\psi_0/\psi_-^*)}{\pi},\quad (12)$$

where $\psi_-^* = 2(1 - \sqrt{1 + \tilde{m}^*/m_{max}}) < 0$ and $\tilde{m}^* = \sqrt{\tilde{\Lambda}_1(0)}/2$ (Equation 20). Second, when the mutational variance, λ , is very small relative to maladaptation, implying that mutants far from $m = 0$ substantially contribute, we find the rate of subcritical 2-step rescue to be nearly

$$\Lambda_2^{(-)}(m_0) \approx -U^2\frac{(1 - \psi_0/2)^{1-n}}{1 - \psi_0/4}\left(e^{-\alpha}\frac{1}{(\alpha/2)^3\pi}\right)^{1/2}.\quad (13)$$

These two approximations do well compared with numerical integration of $\Lambda_2^{(-)}(m_0)$ (Equation 8; see Figure 5 and File S1). As expected, we find that Equation 13 does better under fast wildtype decline while Equation 12 does better when the wildtype is declining more slowly.

For supercritical 2-step rescue, only first-step mutants with growth rates near m^* will contribute (larger m will rescue themselves and are also less likely to arise by mutation), and so we can capture the entire distribution with a small m approximation (following the same approach that led to Equation 12). As shown in File S1, this approximation works well for sufficiently small first-step mutant growth rates, $\psi < \sqrt{2/\rho_{max}}$, beyond which the rate of 2-step rescue through such first-step mutants falls off very quickly due to a lack of mutational input. Thus, considering only supercritical single mutants with scaled growth rate less than $\sqrt{2/\rho_{max}}$, our approximation is

$$\Lambda_2^{(+)}(m_0) \approx U^2\frac{(1 - \psi_0/2)^{1-n}}{1 - \psi_0/4}e^{-\alpha}\frac{\log(\psi_{max}/\psi_+^*)}{\pi},\quad (14)$$

with $\psi_+^* = 2(1 - \sqrt{1 - \tilde{m}^*/m_{max}})$ and $\psi_{max} = \sqrt{2/\rho_{max}}$. This approximation tends to provide a slight overestimate of $\Lambda_2^{(+)}(m_0)$ (Equation 8; see Figure 5 and File S1).

Comparing 2-step regimes These rough but simple closed-form approximations (Equations 11–14) show that, while the contribution of critical mutants to 2-step rescue scales with U^2 , the contribution of non-critical single mutants scales at a rate less than U^2 (Figure 5B) due to a decrease in ψ_-^* (decreasing the range of subcritical mutants) and an increase in ψ_+^* (decreasing the range of supercritical mutants) with U . This difference in scaling with U is stronger when the wildtype is not very maladapted relative to the mutational variance, i.e., when Equation 12 is the better approximation for subcritical rescue. The approximations also show that when initial maladaptation is small, the ratio of supercritical to subcritical contributions (Equation 12 divided by 14) primarily depends on the range of growth rates included in each regime, while with larger initial maladaptation this ratio (Equation 13 divided by 14) begins to depend more strongly on initial maladaptation and mutational variance (α). The effect of maladaptation and mutation rate on the relative contributions of each regime is shown in Figure 5.

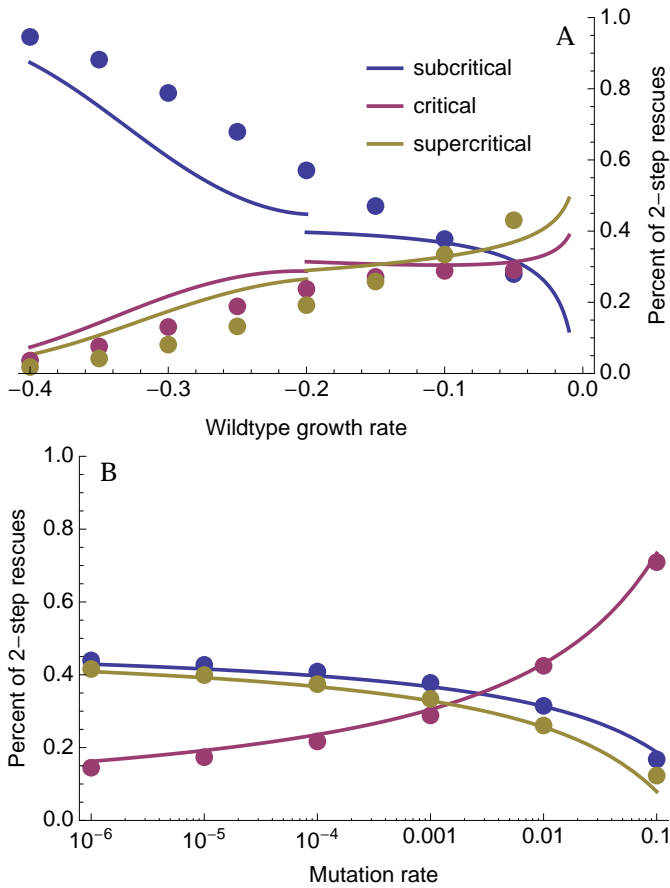


Figure 5 The relative contribution of sufficiently subcritical, critical, and supercritical single mutants to 2-step rescue. The curves are drawn using Equations 10–14 (Equation 12 is used for $m_0 < 0.2$ while Equation 13 is used for $m_0 > 0.2$). The dots are numerical evaluations of Equation 8. Parameters: $n = 4$, $\lambda = 0.005$, $m_{max} = 0.5$, (A) $U = 10^{-3}$, (B) $m_0 = -0.1$.

The distribution of growth rates among rescue genotypes

We next explore the distribution of growth rates among rescue genotypes, i.e., the distribution of growth rates that we expect to observe among the survivors across many replicates.

We begin with 1-step rescue. The rate of 1-step rescue by genotypes with growth rate m is simply $Uf(m|m_0)p_{est}(m)$. Dividing this by the rate of 1-step rescue through any m (Equation 5) gives the distribution of growth rates among the survivors

$$g_1(m) = \frac{Uf(m|m_0)p_{est}(m)}{\Lambda_1(m_0)}, \quad (15)$$

where the mutation rate, U , cancels out. This distribution is shown in blue in Figure 6. The distribution has a mode at small but positive m as a result of two conflicting processes: smaller growth rates are more likely to arise from a declining wildtype but larger growth rates are more likely to establish given they arise. As the rate of wildtype decline increases, the former process exerts more influence, causing the mode to move towards zero and reducing the variance.

We can also give a simple, nearly closed-form approximation here using the same approach taken to reach Equation 19. On the ψ scale, the distribution of effects among 1-step rescue mutations is

$$\tilde{g}_1(\psi) = \frac{\exp(\alpha)\sqrt{\alpha\rho_{max}}}{[\exp(\alpha)\sqrt{\pi\alpha}\text{Erfc}(\sqrt{\alpha}) - 1]\psi_0} e^{-\rho_{max}(\psi-\psi_0)^2/4}\psi, \quad (16)$$

implying the ψ are distributed like a normal truncated below $\psi = 0$ and weighted by ψ . This often provides a very good approximation (see dashed blue curves in Figure 6).

In 2-step rescue, the rate of rescue by double mutants with growth rate m_2 is given by Equation 6 with $\Lambda_1(m)$ replaced by $Uf(m_2|m)p_{est}(m_2)$. Normalizing gives the distribution of growth rates among the double mutant genotypes that rescue the population

$$g_2(m_2) \approx \frac{A(m_2)}{\int_0^{m_{max}} A(m_2)dm_2}$$

$$A(m_2) = \int_{-\infty}^{m_{max}} f(m|m_0)[1 - p_{est}(m)] p(m, Uf(m_2|m)p_{est}(m_2))dm. \quad (17)$$

This distribution, $g_2(m)$, is shown in red in Figure 6. Because the first-step mutants contributing to 2-step rescue tend to be nearer the optimum than the wildtype, this allows them to produce double mutant rescue genotypes with higher growth rates than in 1-step rescue (as seen by comparing the mode between blue and red curves in Figure 6). The fact that these first-step mutants are closer to the optimum also allows for a greater variance in the growth rates of rescue genotypes than in 1-step rescue. Thus the 2-step distribution maintains a more similar mode and variance across wildtype decline rates than the 1-step distribution. Note that because $g_2(m_2)$ depends on U the buffering effect of first-step mutants depends on the mutation rate (see The distribution of growth rates among rescue intermediates below for more discussion).

The distribution of growth rates among rescue intermediates

Finally, our analyses above readily allow us to explore the distribution of first-step mutant growth rates that contribute to 2-step rescue. Analogously to Equation 15, we drop the integral in $\Lambda_2(m_0)$ (Equation 6) and normalize, giving

$$h(m) = \frac{Uf(m|m_0)[1 - p_{est}(m)]p(m, \Lambda_1(m))}{\Lambda_2(m_0)}, \quad (18)$$

where the first U cancels but the U within $\Lambda_1(m)$ does not. This distribution is shown in black in Figure 7. At slow wildtype decline rates the overwhelming majority of 2-step rescue events arise from first-step mutants with growth rates near 0. As indicated by Equation 8, the contribution of first-step mutants with growth rate m declines as $\sim 1/|m|$ as m departs from zero, due to shorter persistence times given eventual extinction. As wildtype growth rate declines, the relative importance of mutational input, $f(m|m_0)$, grows, causing the distribution to flatten and first-step mutants with substantially negative growth rates begin to contribute (compare panels in Figure 7; see also Figure 5A). Decreasing the mutation rate disproportionately increases the contribution of first-step mutants with growth rates near zero (while simultaneously shrinking the range of growth rates that are sufficiently critical; Figure 5B) making the distribution of first-step mutant growth rates contributing to 2-step rescue more sharply peaked around $m = 0$ (Figure S2). Correspondingly, with a higher mutation rate a greater proportion of the contributing single mutants have substantially negative growth rates.

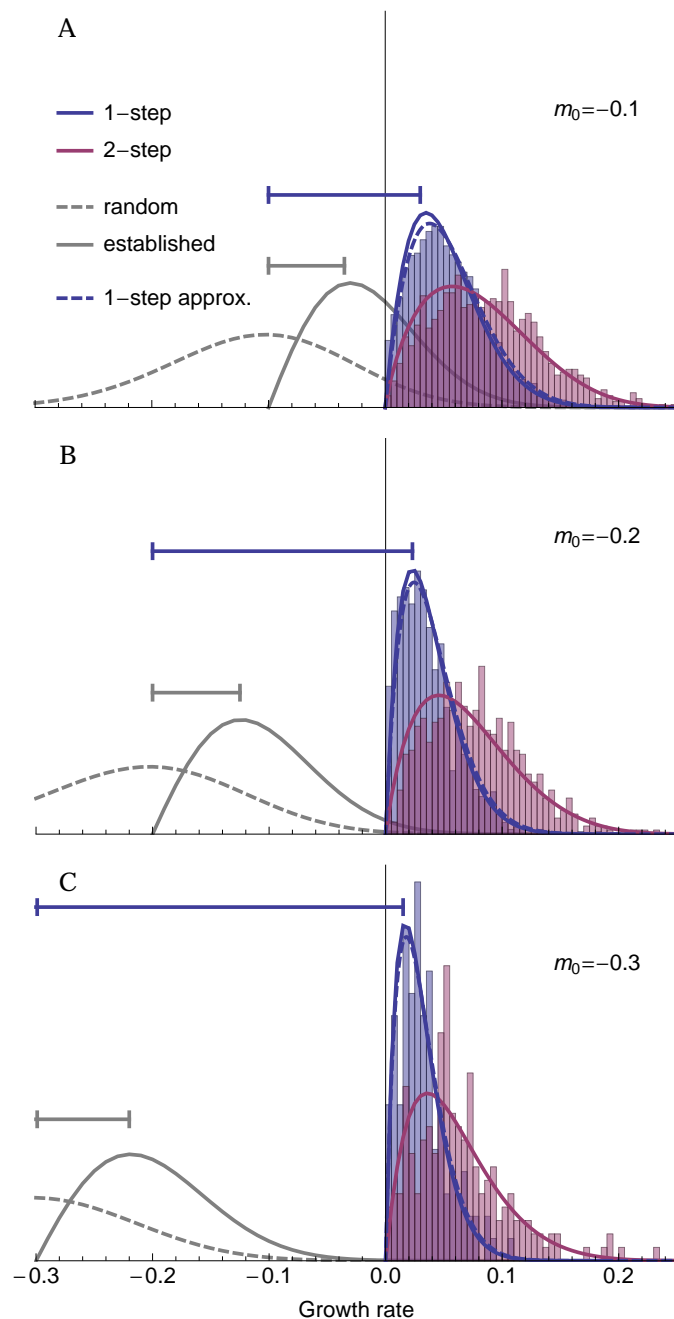


Figure 6 The distribution of growth rates among rescue genotypes under 1-step (blue; Equation 15 solid and 16 dashed) and 2-step (red; Equation 17) rescue for three different levels of initial maladaptation. For comparison, the distribution of random mutations (dashed; Equation 1) and the distribution of beneficial mutations that establish in a population of constant size (solid grey; Equation 1 times Equation 4 and normalized) are shown. Intervals (horizontal lines) indicate the size of the most common fitness effect ($s = m_0 - m$) in a population of constant size (grey) and in 1-step rescue (blue). The histograms show the distribution of growth rates among rescue genotypes observed across (A) 10^4 , (B) 10^5 , and (C) 10^6 simulated replicates. Other parameters: $N_0 = 10^4$, $U = 2 \times 10^{-3}$, $n = 4$, $\lambda = 0.005$, $m_{max} = 0.5$.

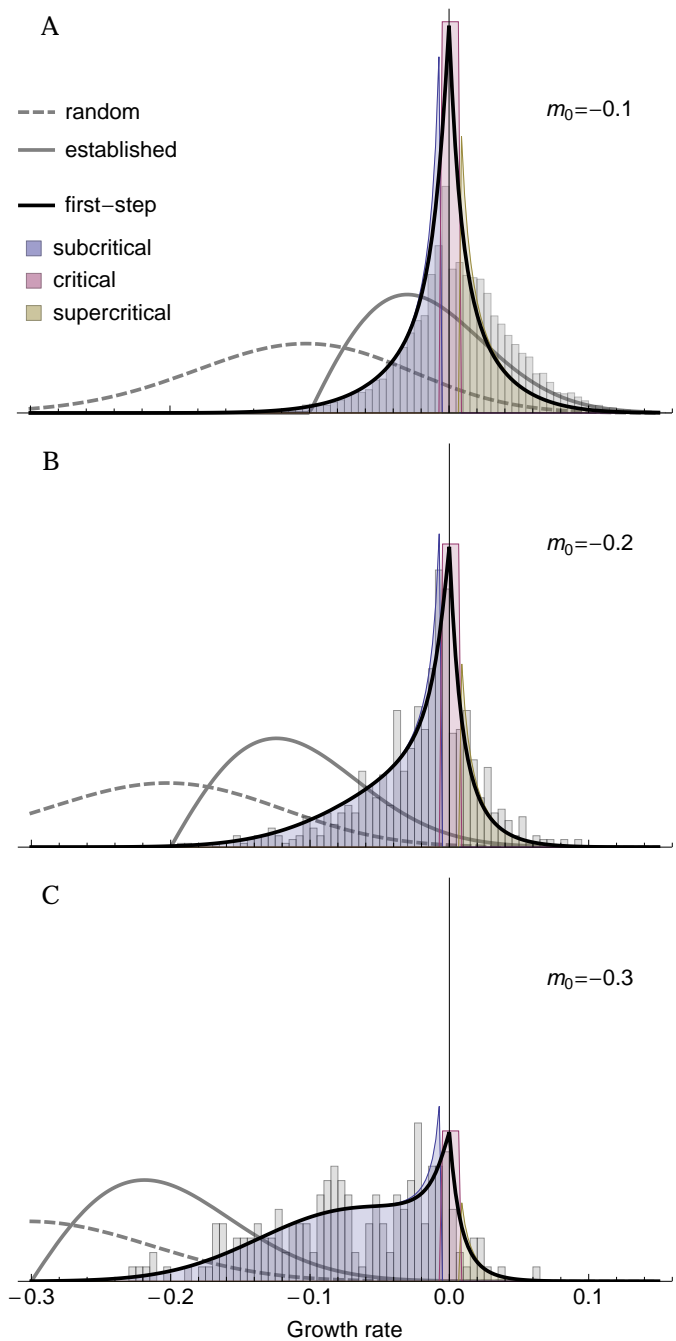


Figure 7 The distribution of growth rates among first-step mutations that lead to 2-step rescue (black; Equation 18) for three different levels of initial maladaptation. Shading represents our sufficiently subcritical approximation (blue; replacing $p(m, \Lambda_1(m))$ with $\Lambda_1(m)/|m|$ in the numerator of Equation 18), our sufficiently critical approximation (red; using $Uf(0|m_0)\sqrt{2\Lambda_1(0)}$ as the numerator in Equation 18), and our sufficiently supercritical approximation (yellow; replacing $p(m, \Lambda_1(m))$ with $\Lambda_1(m)/|m|$ in the numerator of Equation 18). The histograms show the distribution of growth rates among first-step mutations in rescue genotypes with 2 mutations observed across (A, B) 10^5 or (C) 10^6 simulated replicates. We hypothesize that the overabundance of supercriticals (especially in panel A) is likely due to us sampling only the most common rescue genotype in each replicate, which is not necessarily the first genotype that rescues. See Figure 6 for additional details.

Discussion

Here we have explored the probability and genetic basis of evolutionary rescue by multiple mutations on a simple fitness landscape. We find that rescue by multiple mutations can be the most likely path to persistence under high mutation rates or when the population is initially very maladapted. Under these scenarios, intermediate genotypes that are declining less quickly provide a ‘springboard’ from which rescue genotypes emerge. In 2-step rescue these springboard single mutants come from one of three regimes: those that have growth rates near enough to zero (“sufficiently critical”) that rescue is most likely when a mutation persists for an unusually long period of time and grows to an unusually large subpopulation size, and those with growth rates that are either negative or positive enough (“sufficiently subcritical” or “sufficiently supercritical”, respectively) to restrict persistence times and subpopulation sizes, conditioned upon the loss of the first mutation in the absence of a second, rescuing mutation. The relative contribution of each regime shifts with initial maladaptation and mutation rate; rare mutations that can occasionally reach unusually large subpopulation sizes play a larger role when the population is not severely maladapted (e.g., Figure 7A) or mutation rate is high (e.g., Figure S2C). In contrast, when populations are initially very maladapted (e.g., Figure 7C), most first-step mutations are themselves also very maladapted and thus restricted in the subpopulation sizes they are expected to reach before being lost. All three regimes help to maintain the variance in the distribution of fitness effects among rescue genotypes as initial maladaptation increases; meanwhile, in 1-step rescue the variance declines due to ever more extreme sampling of the tail of the mutational distribution (compare blue and red curves in Figure 6).

Our prediction, that rescue by more *de novo* mutations can be more likely than rescue by fewer, is novel. In previous models (e.g., Antia *et al.* 2003; Iwasa *et al.* 2004a; Alexander and Day 2010) the general conclusion has been that, since the probability of rescue scales with U^k (where U is the mutation rate and k is the minimum number of mutations required for rescue), the probability of rescue declines with the number of mutations. This assumes, however, that the probability of a mutation occurring, U , is the limiting factor. Here we have shown that when the probability of a beneficial mutation arising declines with its selective advantage, the probability of sampling once from the extreme tail of the DFE can be lower than sampling multiple mutations closer to the bulk of the DFE, so that rescue via multiple mutations can become the dominant path. Rescue by multiple mutations may also be more likely with standing genetic variation, as small-effect intermediate mutations may segregate at higher frequencies than large-effect rescue mutations before the environmental change (and also decline less quickly than the wildtype following environmental change); this is especially true with recombination, where rescue genotypes can arise from segregating intermediate mutations without mutation (Uecker and Hermisson 2016).

How often rescue arises as a result of multiple mutations is an open question. It is clear that more than one mutation can contribute to adaptation to near-lethal stress, but experiments are often designed to avoid extinction (reviewed in Cowen *et al.* 2002) and therefore greatly expand the scope for multiple mutations to arise on a single genotype. A few exceptions provide some insight. For example, populations of *Saccharomyces cerevisiae* that survived high concentrations of copper acquired multiple mutations (Gerstein *et al.* 2015) – in fact the authors argue for

the ‘springboard effect’ discussed above, where first-step mutations prolong persistence and thereby allow further mutations to arise. In *Pseudomonas fluorescens*, fluctuation tests with nalidixic acid showed that nearly a third of the most resistant surviving strains were double mutants (Bataillon *et al.* 2011), which were able to tolerate 10x higher drug concentrations than single mutants, suggesting 2-step rescue might dominate at high drug concentrations. While suggestive, it is unclear if our prediction – that rescue takes more mutational steps with greater initial maladaptation – holds true generally. Verification will require more experiments that allow extinction and uncover the genetic basis of adaptation at different severities of environmental change (e.g., drug concentration).

In describing the genetic basis of adaptation in populations of constant size, Orr (1998) showed that the mean phenotypic displacement towards the optimum scales roughly linearly with initial displacement. Converting phenotype to fitness, this implies that the mean fitness effect of fixed mutations ($s = m - m_0$) increases exponentially as initial Malthusian fitness (m_0) declines (i.e., $s \sim \exp(-m_0)$), which is a roughly linear increase when initial fitness is small ($|m_0| \ll 1$). Here we see that, under 1-step rescue, the mean fitness effect also increases roughly linearly as the initial growth rate declines (see horizontal blue lines in Figure 6). However, the rate of this linear increase in fitness effect is much larger under rescue than in a population of constant size (compare blue and grey horizontal lines in Figure 6), where declines in wildtype fitness not only allow larger mutations to be beneficial but also require larger mutations for persistence. Thus the race between extinction and adaptation during evolutionary rescue is expected to produce a genetic basis of adaptation with fewer mutations of larger effect.

While under 1-step rescue the fitness effect of the first mutation increases roughly linearly as wildtype fitness declines, most rescue events will be 2-step for wildtype fitnesses below some value (e.g., at $m_0 \approx -0.25$ in Figure 3; this threshold value of m_0 increases with mutation rate, Figure S1). At this junction the effect size of the first mutation will no longer increase as quickly (and potentially even decrease), as it switches from a rescue mutant to an intermediate mutant whose expected fitness begins to decline substantially with the fitness of the wildtype (Figure 7). Thus as rescue switches from dominantly k -step to dominantly $(k + 1)$ -step the genetic basis of adaptation becomes more diffuse, with each mutation having a smaller individual fitness effect as the contributing fitness effects spread over more loci. In the limit of large k (due to large initial maladaptation or high mutation rates), the genetic basis of adaptation should at some point converge to many loci with small effect, as would also be expected in a population of constant size. Indeed, at very high mutation rates the rate of adaptation (the change in mean fitness) is the same under rescue as it is in populations of constant size (Anciaux *et al.* 2019), implying that the genetic basis of adaptation no longer depends on demography. It is therefore at intermediate levels of initial maladaptation and low mutation rates, where rescue primarily occurs from a few large effect mutations, that the race between adaptation and persistence is predicted to have the largest effect on the genetic basis of adaptation.

Fluctuation tests (Luria and Delbrück 1943) provide a means to generate random mutations and then isolate potential rescue genotypes (typically assumed to be 1-step only), whose growth rates can be measured under the selective conditions. These experiments are designed such that there is substantial standing

837 genetic variation at the time of exposure to the selective con- 899
838 ditions, which should increase the contributions of mutations 900
839 with small growth rates (Orr and Betancourt 2001), although 901
840 these could be outcompeted by mutations with higher growth 902
841 rates and/or be under-sampled. Regardless, consistent with 903
842 our theory (Figure 6), the resulting growth rate distributions 904
843 in both bacteria and yeast often find modes that are substantially 905
844 greater than zero (as opposed to, say, an exponential distribution; 906
845 Kassen and Bataillon 2006; MacLean and Buckling 2009; Gerstein 907
846 *et al.* 2012; Lindsey *et al.* 2013; Gerstein *et al.* 2015). A number of 908
847 these conform even more closely to our expected shape (Kassen 909
848 and Bataillon 2006; Gerstein *et al.* 2015) while the others appear 910
849 to be substantially more clumped around the mode, perhaps 911
850 due to a very restricted number of possible rescue mutations in 912
851 any one circumstance, the size of the experiment, or the way in 913
852 which growth rates are measured. Finally, Gerstein *et al.* (2015) 914
853 not only provide the distribution of growth rates among rescue 915
854 genotypes, but also the growth rates of individual mutations 916
855 that compose multi-step rescue genotypes. In four lines where 917
856 multiple mutations were detected and a segregation analysis 918
857 performed, one mutation in each line was inferred to have a 919
858 minor effect and the other mutation was an amplification of the 920
859 copper metallothionein CUP with a major fitness effect. These 921
860 results are consistent with the minor effect mutations being sub-
861 critical mutations that provided a springboard for the larger
862 CUP mutations.

863 Pinpointing the mutations responsible for adaptation is ham-
864 pered by genetic hitchhiking, as beneficial alleles elevate the fre-
865 quency of linked neutral and mildly deleterious alleles (Barton
866 2000). The problem is particularly severe under strong selection
867 and low recombination, and therefore reaches an extreme in
868 the case of evolutionary rescue in asexuals, especially if many
869 neutral and deleterious mutations are segregating at the time
870 of environmental change. To circumvent this, mutations that
871 have risen to high frequency in multiple replicates are often in-
872 troduced in a wildtype background, in isolation and sometimes
873 also in combination with a small number of other common high-
874 frequency mutations, and grown under the selective conditions
875 (e.g., Jochumsen *et al.* 2016; Ono *et al.* 2017). As we have demon-
876 strated above (e.g., Figure 7C), however, under multi-step rescue
877 there may be no one mutation that individually confers growth
878 in the selective conditions. Thus, a mutation that was essential
879 for rescue may go undetected or be mistaken as a hitchhiker if
880 the appropriate multiple-mutation genotypes are not tested. Un-
881 fortunately reverse engineering all combinations of mutations
882 quickly becomes unwieldy as the number of mutations grows,
883 and thus this approach will not be practical under severe initial
884 maladaptation and high mutation rates, where we predict rescue
885 to occur by many mutations. Interestingly, our simulations show
886 that the population dynamics themselves may help differentiate
887 how many mutations contribute to rescue (e.g., V- vs. U-shaped
888 log-trajectories; Figures 1 and 2), and fitting models of k -step
889 rescue could produce estimates for the growth rates of the k
890 genotypes.

891 Environmental change often selects for mutator alleles, which
892 elevate the rate at which beneficial alleles arise and subsequently
893 increase in frequency with them (Tenaillon *et al.* 2001). When
894 beneficial alleles are required for persistence, as in evolution-
895 ary rescue, mutator alleles can reach very high frequencies or
896 rapidly fix (e.g., Mao *et al.* 1997). Consistent with this, mutator
897 alleles are often associated with antibiotic resistance in clinical
898 isolates (see examples in Bell 2017). Further, the more benefi-

900 cial mutations available the larger the advantage of a mutator
901 allele; for a mutator that increases the mutation rate m -fold, its
902 relative contribution to the production of n beneficial mutations
903 scales as m^n (Tenaillon *et al.* 1999). Thus, conditions that cause
904 multi-step rescue to be more likely than 1-step rescue should
905 also impose stronger selection for mutator alleles. There are a
906 number of examples where lineages with higher mutation rates
907 acquired multiple mutations and persisted at higher doses of an-
908 tibiotics (Couce *et al.* 2015; San Millan *et al.* 2017). The number of
909 mutations required for persistence is, however, often unknown,
910 making it difficult to compare situations where rescue requires
911 different numbers of mutations. Experiments with a combina-
912 tion of drugs may provide a glimpse; for instance, *Escherichia*
913 *coli* populations only evolved resistance to a combination of two
914 drugs (presumably through the well-known mutations specific
915 to each drug) when mutators were present, despite the fact that
916 mutators were not required for resistance to either drug in isola-
917 tion (Gifford *et al.* 2019). In cases where we have less information
918 on the genetic basis of resistance, our model suggests that muta-
919 tors will be more advantageous when initial maladaptation is
920 severe (e.g., higher drug concentrations or a larger number of
921 drugs), as rescue will then be dominated by genetic paths with
922 more mutational steps.

923 Here we have investigated the genetic basis of evolution-
924 ary rescue in an asexual population that is initially genetically
925 uniform. Extending this work to allow for recombination and
926 standing genetic variation at the time of environmental change
927 – as expected for many natural populations – would be valu-
928 able. The effect of standing genetic variation on the probability
929 of 1-step rescue is relatively straight-forward to incorporate,
930 depending only on the expected number of rescue mutations
931 initially present and their mean establishment probability (Mar-
932 tin *et al.* 2013). In the case of the fluctuation tests discussed
933 above, where mutations accumulated in the short interval before
934 the onset of selection are assumed to be relatively neutral, the
935 effect of standing genetic variance on 1-step rescue might
936 be incorporated by a simple rescaling of N_0 , to account for the
937 additional mutants present in the standing variation. When
938 considering longer periods of time in populations that are not
939 rapidly expanding, mutation-selection balance may be reached
940 before the onset of selection. In this case the probability of 1-
941 step rescue from standing genetic variance in Fisher’s geometric
942 model was given by Anciaux *et al.* (2018), whose equations 3
943 and 5 immediately give the distribution of fitness effects among
944 those that rescue. Allowing these standing genetic variants to
945 be springboards to multi-step rescue will help clarify the role of
946 standing genetic variation on the genetic basis of rescue more
947 generally. Recombination can help combine such springboard
948 mutations into rescue genotypes but will also break these combi-
949 nations apart, as demonstrated in a 2-locus 2-allele model of
950 rescue (Uecker and Hermisson 2016). How recombination af-
951 fects the genetic basis of evolutionary rescue when more loci can
952 potentially contribute remains to be seen. Also left unexplored
953 is the effect of density-dependent fitness; for example, competi-
954 tion may reduce mutant growth rates and thereby increase the
955 size of mutations that are required for rescue, especially when
956 the wildtype declines slowly. Combining density-dependence
957 and standing genetic variance is known to create complex dy-
958 namics in a 1-locus 2-allele model of rescue (Uecker *et al.* 2014),
959 and adding more potential genotypes is sure to add yet more
960 complexity.

Many of our simple closed-form results rely upon knowing

961 the distribution of mutant growth rates (Equation 1), which 1023
962 arises from the assumption that mutant phenotypes are nor- 1024
963 mally distributed about their ancestor and Malthusian fitness 1025
964 is a quadratic, on some scaled phenotypic axes. It is clear that 1026
965 deviations from these assumptions will, at least quantitatively, 1027
966 affect our results. For instance, mutant phenotype distributions 1028
967 with truncated or fat tails are likely to lead to smaller or larger 1029
968 mutational steps, respectively, with downstream effects on the 1030
969 probability of rescue, the number of contributing mutations, and 1031
970 the resulting DFEs. As a preliminary investigation of this pre- 1032
971 diction, we have performed simulations with mutant phenotype 1033
972 distributions having the same expectation and covariances as 1034
973 assumed above under normality, but with truncated (platykur- 1035
974 tic) or fat (leptokurtic) tails (Figure S3A). While our qualitative 1036
975 results above hold, the probability of rescue declines slower with 1037
976 wildtype maladaptation when the mutational distribution has 1038
977 fatter tails (compare dotted and solid black in Figure S3C). Fatter 1039
978 tails also reduce the number of mutations contributing to rescue 1040
979 (e.g., 1-step rescue dominates for all wildtype decline rates in 1041
980 Figure S3C). Finally, fatter tails cause the distributions of rescue 1042
981 genotype growth rates following 1- and 2-step rescue to have 1043
982 more variance and become more similar to one another (Figure 1044
983 S4B) and also tend to increase the contribution of supercritical 1045
984 single mutants in 2-step rescue (Figure S5). All told, the genetic 1046
985 basis of rescue is expected to consist of fewer mutations of larger 1047
986 effect, with less consistent effect sizes across replicate popula- 1048
987 tions, as the tails of the mutant phenotype distribution become 1049
988 fatter. 1050

989 In the numerical examples above we have not varied the 1051
990 number of scaled phenotypic axes, n , i.e., the dimensionality of 1052
991 the phenotypic landscape (although the analytical results apply 1053
992 for arbitrary n). Because increasing the number of dimensions 1054
993 changes the distribution of fitness effects, and in particular de- 1055
994 creases the proportion of mutations that are beneficial (Fisher 1056
995 1930), this may have cascading influences on our results. As 1057
996 shown in Anciaux *et al.* (2018), the probability of 1-step rescue 1058
997 by *de novo* mutation declines with dimensionality, and is only 1059
998 weakly dependent on dimensionality when initial maladaptation 1060
999 is small (such that $\Lambda_1(m_0) \approx -m_0 U g(\alpha)$, Equation 19). 1061
1000 Here we show that the distribution of fitness effects among 1- 1062
1001 step rescue mutants is nearly independent of dimensionality for 1063
1002 any degree of initial maladaptation (Equation 16 and the blue 1064
1003 curves in Figure S6B). Further, as seen by comparing Equations 1065
1004 11-14 to Equation 19, the probability of 2-step rescue depends 1066
1005 on dimensionality much like 1-step rescue does, suggesting that 1067
1006 while increasing dimensionality may decrease the probability 1068
1007 of rescue it may have little effect on the number of steps rescue 1069
1008 tends to take. This is demonstrated more generally in Figure 1070
1009 S6A, where an order of magnitude increase in the number of 1071
1010 dimensions decreases the probability of rescue by roughly an 1072
1011 order of magnitude but has little effect on the relative rates of 1-, 1073
1012 2-, 3-, and 4-step rescue. Finally, Figure S6B-C shows that dimen- 1074
1013 sionality has very little effect on the distribution of fitness effects 1075
1014 among 2-step rescue genotypes (Equation 17) and among first 1076
1015 step mutants leading to 2-step rescue (Equation 18). To conclude, 1077
1016 while the probability of rescue declines with the complexity of 1078
1017 the organism and its environment, the genetic basis of rescue is 1079
1018 expected to be relatively invariant across complexity, as with the 1080
1019 genetic basis of adaptation in populations of constant size (Orr 1081
1020 1998, see also gray curves in Figure S6B,C).

1021 In the numerical examples above we have also focused on a 1080
1022 particular value of mutational variance, λ . Clearly, since rescue 1081

relies on mutations of large effect, decreasing λ should decrease 1082
the probability of rescue, much like decreasing the mutation rate, 1083
 U , does (Figure S1). While our analysis (Equations 19 and 11-14) 1084
and numerical results (see File S1) show that this is true, we find 1085
that λ and U have very different effects on the genetic basis of 1086
rescue (File S1). In particular, given a similar effect on the total 1087
probability of rescue, decreasing U generally restricts rescue to 1088
fewer mutational steps while decreasing λ forces rescue to occur 1089
by more mutations. Further, the distribution of fitness effects 1090
of mutations contributing to rescue is nearly independent of 1091
 U but a decrease in λ strongly reduces the mode of the DFE. 1092
This demonstrates that populations with similar probabilities of 1093
rescue can vary greatly in the way they achieve it genetically. 1094

1036 Acknowledgements

1037 We would like to thank the Otto and Doebeli labs for helpful 1038
1039 feedback at various stages, Ophélie Ronce and Thomas Lenor- 1040
1041 mand for their hospitality and valuable input at the beginning 1042
1043 of this project, and Mike Whitlock, Amy Angert, Luis-Miguel 1044
1045 Chevin, and Joachim Hermisson for constructive criticism on 1046
1047 previous versions of the manuscript. Funding provided by the 1048
1049 National Science and Engineering Research Council (CGS-D 1050
1051 6564 to M.M.O., RGPIN-2016-03711 to S.P.O.), the University 1052
1053 of British Columbia, Banting, and the University of California 1054
1055 - Davis (fellowships to M.M.O.), the National Institute of Gen- 1056
1057 eral Medical Sciences of the National Institutes of Health (NIH 1057
1058 R01 GM108779 to Graham Coop), the Agence Nationale de la 1059
1060 Recherche (ANR-18-CE45-0019 "RESISTE" to G.M.), and the Cen- 1061
1062 tre Méditerranéen Environment et Biodiversité ("BACTPHI" to 1062
1063 G.M.). 1064

1052 Literature Cited

- 1053 Abramowitz, M. and I. A. Stegun, editors, 1972 *Handbook of*
1054 *mathematical functions with formulas, graphs, and mathematical*
1055 *tables*. United States Department of Commerce, Washington,
1056 DC, USA.
1057 Alexander, H. K. and T. Day, 2010 Risk factors for the evolu-
1058 tionary emergence of pathogens. *Journal of the Royal Society*
1059 *Interface* 7: 1455–1474.
1060 Alexander, H. K., G. Martin, O. Y. Martin, and S. Bonhoeffer,
1061 2014 Evolutionary rescue: linking theory for conservation and
1062 medicine. *Evolutionary Applications* 7: 1161–1179.
1063 Allen, L. J., 2010 *An introduction to stochastic processes with appli-*
1064 *cations to biology*. CRC Press.
1065 Anciaux, Y., L.-M. Chevin, O. Ronce, and G. Martin, 2018 Evolu-
1066 tionary rescue over a fitness landscape. *Genetics* 209: 265–279.
1067 Anciaux, Y., A. Lambert, O. Ronce, L. Roques, and G. Martin,
1068 2019 Population persistence under high mutation rate: from
1069 evolutionary rescue to lethal mutagenesis. *Evolution* .
1070 Antia, R., R. R. Regoes, J. C. Koella, and C. T. Bergstrom, 2003
1071 The role of evolution in the emergence of infectious diseases.
1072 *Nature* 426: 658.
1073 Barton, N. H., 2000 Genetic hitchhiking. *Philosophical Trans-*
1074 *actions of the Royal Society of London. Series B: Biological*
1075 *Sciences* 355: 1553–1562.
1076 Bataillon, T. and S. F. Bailey, 2014 Effects of new mutations on
1077 fitness: Insights from models and data. *Annals of the New*
1078 *York Academy of Sciences* 1320: 76–92.
1079 Bataillon, T., T. Zhang, and R. Kassen, 2011 Cost of adaptation
1080 and fitness effects of beneficial mutations in *Pseudomonas*
1081 *fluorescens*. *Genetics* 189: 939–949.

- 1082 Bell, G., 2009 The oligogenic view of adaptation. *Cold Spring* 1144
1083 *Harbor Symposia on Quantitative Biology* **74**: 139–144. 1145
- 1084 Bell, G., 2017 Evolutionary rescue. *Annual Review of Ecology,* 1146
1085 *Evolution, and Systematics* **48**: 605–627. 1147
- 1086 Couce, A., A. Rodríguez-Rojas, and J. Blázquez, 2015 Bypass 1148
1087 of genetic constraints during mutator evolution to antibiotic 1149
1088 resistance. *Proceedings of the Royal Society B: Biological Sci-* 1150
1089 *ences* **282**: 20142698. 1151
- 1090 Cowen, L. E., J. B. Anderson, and L. M. Kohn, 2002 Evolution 1152
1091 of drug resistance in *Candida albicans*. *Annual Reviews in* 1153
1092 *Microbiology* **56**: 139–165. 1154
- 1093 Dettman, J. R., N. Rodrigue, A. H. Melnyk, A. Wong, S. F. Bailey, 1155
1094 *et al.*, 2012 Evolutionary insight from whole-genome sequenc- 1156
1095 ing of experimentally evolved microbes. *Molecular ecology* 1157
1096 **21**: 2058–2077. 1158
- 1097 Fisher, R. A., 1918 The correlation between relatives on the sup- 1159
1098 position of mendelian inheritance. *Transactions of the Royal* 1160
1099 *Society of Edinburgh* **52**: 399–433. 1161
- 1100 Fisher, R. A., 1930 *The genetical theory of natural selection*. Claren- 1162
1101 don Press, London. 1163
- 1102 Gerstein, A. C., D. S. Lo, and S. P. Otto, 2012 Parallel genetic 1164
1103 changes and nonparallel gene–environment interactions char- 1165
1104 acterize the evolution of drug resistance in yeast. *Genetics* **192**: 1166
1105 241–252. 1167
- 1106 Gerstein, A. C., J. Ono, D. S. Lo, M. L. Campbell, A. Kuzmin, 1168
1107 *et al.*, 2015 Too much of a good thing: the unique and repeated 1169
1108 paths toward copper adaptation. *Genetics* **199**: 555–571. 1170
- 1109 Gifford, D. R., E. Berríos-Caro, C. Joerres, T. Galla, and C. G. 1171
1110 Knight, 2019 Mutators drive evolution of multi-resistance to 1172
1111 antibiotics. *bioRxiv* p. 643585. 1173
- 1112 Gomulkiewicz, R. and R. D. Holt, 1995 When does evolution by 1174
1113 natural selection prevent extinction? *Evolution* **49**: 201–207. 1175
- 1114 Haldane, J. B. S., 1927 A Mathematical Theory of Natural and 1176
1115 Artificial Selection, Part V: Selection and Mutation. *Mathemat-* 1177
1116 *ical Proceedings of the Cambridge Philosophical Society* **23**: 1178
1117 838. 1179
- 1118 Harmand, N., R. Gallet, R. Jabbour-Zahab, G. Martin, and 1180
1119 T. Lenormand, 2017 Fisher’s geometrical model and the muta- 1181
1120 tional patterns of antibiotic resistance across dose gradients. 1182
1121 *Evolution* **71**: 23–37. 1183
- 1122 Iwasa, Y., F. Michor, and M. A. Nowak, 2004a Evolutionary dy- 1184
1123 namics of invasion and escape. *Journal of Theoretical Biology* 1185
1124 **226**: 205–214. 1186
- 1125 Iwasa, Y., F. Michor, and M. A. Nowak, 2004b Stochastic tunnels 1187
1126 in evolutionary dynamics. *Genetics* **166**: 1571–1579. 1188
- 1127 Jochumsen, N., R. L. Marvig, S. Damkjaer, R. L. Jensen, W. Paulan- 1189
1128 der, *et al.*, 2016 The evolution of antimicrobial peptide res- 1190
1129 sistance in *Pseudomonas aeruginosa* is shaped by strong 1191
1130 epistatic interactions. *Nature communications* **7**: 13002. 1192
- 1131 Kassen, R. and T. Bataillon, 2006 Distribution of fitness effects 1193
1132 among beneficial mutations before selection in experimental 1194
1133 populations of bacteria. *Nature genetics* **38**: 484. 1195
- 1134 Kimura, M., 1965 A stochastic model concerning the mainte- 1196
1135 nance of genetic variability in quantitative characters. *Pro-* 1197
1136 *ceedings of the National Academy of Sciences* **54**: 731–736. 1198
- 1137 Kimura, M., 1983 *The neutral theory of molecular evolution*. Cam- 1199
1138 bridge University Press, Cambridge, UK. 1200
- 1139 Lande, R., 1980 The genetic covariance between characters main- 1201
1140 tained by pleiotropic mutations. *Genetics* **94**: 203–215. 1202
- 1141 Lindsey, H. A., J. Gallie, S. Taylor, and B. Kerr, 2013 Evolution- 1203
1142 ary rescue from extinction is contingent on a lower rate of 1204
1143 environmental change. *Nature* **494**: 463–467. 1205
- Luria, S. E. and M. Delbrück, 1943 Mutations of bacteria from 1144
virus sensitivity to virus resistance. *Genetics* **28**: 491.
- MacLean, R. C. and A. Buckling, 2009 The distribution of fitness 1146
effects of beneficial mutations in *Pseudomonas aeruginosa*. *PLoS*
Genetics **5**: e1000406.
- MacLean, R. C., A. R. Hall, G. G. Perron, and A. Buckling, 2010 1148
The population genetics of antibiotic resistance: integrating 1149
molecular mechanisms and treatment contexts. *Nature Re-* 1150
views Genetics **11**: 405.
- Mao, E. F., L. Lane, J. Lee, and J. H. Miller, 1997 Proliferation 1152
of mutators in a cell population. *Journal of Bacteriology* **179**:
417–422.
- Martin, G., 2014 Fisher’s geometrical model emerges as a prop- 1154
erty of complex integrated phenotypic networks. *Genetics* **197**:
237–255.
- Martin, G., R. Aguilée, J. Ramsayer, O. Kaltz, and O. Ronce, 2013 1156
The probability of evolutionary rescue: towards a quantita- 1157
tive comparison between theory and evolution experiments. 1158
Philosophical Transactions of the Royal Society of London B:
Biological Sciences **368**: 20120088.
- Martin, G. and T. Lenormand, 2006 The fitness effect of muta- 1160
tions across environments: a survey in light of fitness land- 1161
scape models. *Evolution* **60**: 2413–2427.
- Martin, G. and T. Lenormand, 2015 The fitness effect of muta- 1163
tions across environments: Fisher’s geometrical model with 1164
multiple optima. *Evolution* **69**: 1433–1447.
- Martin, G. and L. Roques, 2016 The nonstationary dynamics of 1166
fitness distributions: asexual model with epistasis and stand- 1167
ing variation. *Genetics* **204**: 1541–1558.
- Maruyama, T. and M. Kimura, 1974 A note on the speed of gene 1169
frequency changes in reverse directions in a finite population.
Evolution pp. 161–163.
- Ono, J., A. C. Gerstein, and S. P. Otto, 2017 Widespread genetic 1171
incompatibilities between first-step mutations during parallel 1172
adaptation of *Saccharomyces cerevisiae* to a common environ- 1173
ment. *PLoS biology* **15**: e1002591.
- Orr, H. A., 1998 The Population Genetics of Adaptation: The 1175
Distribution of Factors Fixed during Adaptive Evolution. *Evo-*
lution **52**: 935.
- Orr, H. A., 2005 The genetic theory of adaptation: a brief history. 1177
Nature Reviews Genetics **6**: 119–27.
- Orr, H. A. and A. J. Betancourt, 2001 Haldane’s sieve and adap- 1179
tation from the standing genetic variation. *Genetics* **157**: 875–
884.
- Orr, H. A. and R. L. Unckless, 2014 The population genetics of 1181
evolutionary rescue. *PLoS Genetics* **10**: e1004551.
- Otto, S. P. and M. C. Whitlock, 1997 The probability of fixation 1183
in populations of changing size. *Genetics* **146**: 723–733.
- Pennings, P. S., S. Kryazhinskiy, and J. Wakeley, 2014 Loss and 1185
recovery of genetic diversity in adapting populations of hiv.
PLoS Genetics **10**: e1004000.
- Robbins, N., T. Caplan, and L. E. Cowen, 2017 Molecular evolu- 1187
tion of antifungal drug resistance. *Annual Review of Microbi-*
ology **71**: 753–775.
- San Millan, A., J. A. Escudero, D. R. Gifford, D. Mazel, and R. C. 1189
MacLean, 2017 Multicopy plasmids potentiate the evolution 1190
of antibiotic resistance in bacteria. *Nature ecology & evolution*
1: 0010.
- Schlötterer, C., R. Kofler, E. Versace, R. Tobler, and S. Franssen, 1192
2015 Combining experimental evolution with next-generation 1193
sequencing: a powerful tool to study adaptation from stand- 1194
ing genetic variation. *Heredity* **114**: 431–440.

1206 Stapley, J., J. Reger, P. G. Feulner, C. Smadja, J. Galindo, *et al.*, 1260
 1207 2010 Adaptation genomics: the next generation. Trends in 1261
 1208 ecology & evolution **25**: 705–712. 1262
 1209 Tenaillon, O., 2014 The utility of Fisher’s geometric model in 1263
 1210 evolutionary genetics. Annual Review of Ecology, Evolution, 1264
 1211 and Systematics **45**: 179–201. 1265
 1212 Tenaillon, O., F. Taddei, M. Radman, and I. Matic, 2001 Second- 1266
 1213 order selection in bacterial evolution: selection acting on muta- 1267
 1214 tion and recombination rates in the course of adaptation. 1268
 1215 Research in microbiology **152**: 11–16. 1269
 1216 Tenaillon, O., B. Toupance, H. Le Nagard, F. Taddei, and 1270
 1217 B. Godelle, 1999 Mutators, population size, adaptive land- 1271
 1218 scape and the adaptation of asexual populations of bacteria. 1272
 1219 Genetics **152**: 485–493. 1273
 1220 Turelli, M., 1984 Heritable genetic variation via mutation- 1274
 1221 selection balance: Lerch’s zeta meets the abdominal bristle. 1275
 1222 Theoretical population biology **25**: 138–193. 1276
 1223 Turelli, M., 1985 Effects of pleiotropy on predictions concerning 1277
 1224 mutation-selection balance for polygenic traits. Genetics **111**: 1278
 1225 165–195. 1279
 1226 Uecker, H. and J. Hermisson, 2016 The role of recombination in 1280
 1227 evolutionary rescue. Genetics **202**: 721–732. 1281
 1228 Uecker, H., S. P. Otto, and J. Hermisson, 2014 Evolutionary rescue 1282
 1229 in structured populations. The American Naturalist **183**: E17–
 1230 E35.
 1231 Weinreich, D. M., N. F. Delaney, M. A. DePristo, and D. L. Hartl,
 1232 2006 Darwinian evolution can follow only very few muta- 1283
 1233 tional paths to fitter proteins. science **312**: 111–114. 1284
 1234 Weissman, D. B., M. M. Desai, D. S. Fisher, and M. Feldman, 2009 1285
 1235 The rate at which asexual populations cross fitness valleys. 1286
 1236 Theoretical Population Biology **75**: 286–300. 1287
 1237 Weissman, D. B., M. W. Feldman, and D. S. Fisher, 2010 The rate 1288
 1238 of fitness-valley crossing in sexual populations. Genetics **186**:
 1239 1389–1410. 1289
 1240 Williams, K.-A. and P. S. Pennings, 2019 Drug resistance evolu-
 1241 tion in hiv in the late 1990s: hard sweeps, soft sweeps, clonal
 1242 interference and the accumulation of drug resistance muta-
 1243 tions. BioRxiv p. 548198.
 1244 Wolfram Research Inc., 2012 Mathematica, Version 9.0. Cham-
 1245 paign, IL.
 1246 Yilmaz, N. K., R. Swanstrom, and C. A. Schiffer, 2016 Improving
 1247 viral protease inhibitors to counter drug resistance. Trends in
 1248 Microbiology **24**: 547–557.

1249 Appendix

1250 Approximating the probability of 1-step rescue

1251 The probability of 1-step rescue in this model has been derived
 1252 by [Anciaux *et al.* \(2018\)](#). As replicated in File S1 and given by
 1253 their equation 7, when $\rho_{max} = m_{max}/\lambda$ is large a simple, nearly
 1254 closed-form approximation is

$$1255 \Lambda_1(m_0) \approx \tilde{\Lambda}_1(m_0) \equiv -m_0 U \frac{(1 - \psi_0/2)^{(1-n)/2}}{1 - \psi_0/4} g(\alpha), \quad (19)$$

1256 where $\psi_0 = 2(1 - \sqrt{1 - m_0/m_{max}})$, $g(\alpha) = \exp(-\alpha)/\sqrt{\pi\alpha} -$
 1257 $\operatorname{erfc}(\sqrt{\alpha})$, and $\alpha = \rho_{max}\psi_0^2/4$, with $\operatorname{erfc}(\cdot)$ the complimentary
 1258 error function. When the wildtype declines slowly m_0 and thus
 1259 ψ_0 is small and $\Lambda_1(m_0) \approx Ug(\alpha)$. In the limit $m_0 \rightarrow 0$, Equation
 19 becomes

$$\tilde{\Lambda}_1(0) \equiv \lim_{m_0 \rightarrow 0} \tilde{\Lambda}_1(m_0) = 2U\sqrt{m_{max}\lambda/\pi}. \quad (20)$$

Mutant lineage dynamics

1260 Here we follow the lead of [Weissman *et al.* \(2010\)](#) and [Uecker
 1261 and Hermisson \(2016\)](#) in approximating our discrete-time pro-
 1262 cess with a continuous-time branching process (see chapter 6 in
 1263 [Allen 2010](#)). Consider a birth-death process, where individuals
 1264 give birth at rate b and die at rate d . One can then obtain the
 1265 probability generating function for the number of individuals at
 1266 a given time, $n(t)$, given the initial number, $n(0)$. We are primar-
 1267 ily interested in new mutant lineages, $n(0) = 1$. The generating
 1268 function then allows us to calculate the probability that a lineage
 1269 persists at least until time t and the distribution of $n(t)$ given it
 1270 does so (see below). 1271

To convert between birth and death rates and our compound
 1272 Malthusian parameter we follow [Uecker and Hermisson \(2016\)](#)
 1273 in equally distributing the growth rate m between birth and
 1274 death, $b = (1 + m)/2$ and $d = (1 - m)/2$, such that $m = b - d$
 1275 and the continuous-time process exhibits the same amount of
 1276 drift as the discrete time process (and matches discrete-time
 1277 simulations well; [Uecker *et al.* 2014](#)). We can now report the
 1278 necessary results in terms of m (assuming $|m| < 1$). 1279

Denoting the extinction time as T , the probability a mutant
 1280 with growth rate m persists until time t is approximately (see
 1281 File S1 for derivation) 1282

$$P(T > t) \approx \begin{cases} 2/t & t \ll |1/m| \\ -2m \exp(mt) & t \gg -1/m > 0 \end{cases} \quad (21)$$

As pointed out in [Weissman *et al.* \(2010\)](#) (whose equation A2
 1283 differs from Equation 21 by a factor of 2 because they have
 1284 $b + d = 2$), the distribution of persistence times has a long
 1285 tail (like $1/t$) until being cut off (declining exponentially) at
 1286 $t = -1/m$. 1287

Given a lineage persists until t , the distribution of $n(t)$ is
 1288 roughly (see File S1 for derivation) 1289

$$P(n(t) = n | n(t) > 0) \approx \begin{cases} 2(1/t)(1 + 2/t)^{-n} & t \ll |1/m| \\ -2m(1 + m)^{n-1} & t \gg -1/m > 0 \end{cases} \quad (22)$$

As pointed out in [Weissman *et al.* \(2010\)](#) (whose equation A3
 1290 only differs from Equation 22 by constants), the distribution of
 1291 $n(t)$ is approximately geometric for small or large t , implying
 1292 $n(t)$ is very unlikely to be greater than the minimum of t and
 1293 $-1/m$. 1294

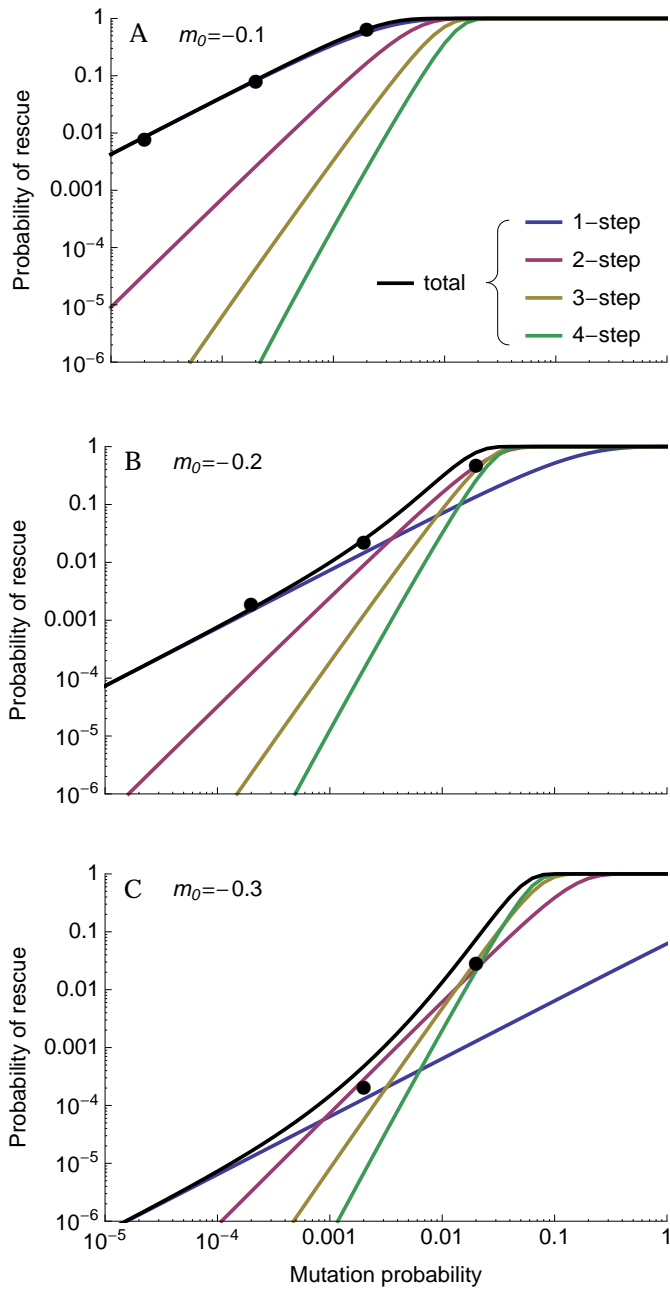


Figure S1 The probability of rescue as a function of mutation rate for three different levels of initial maladaptation. See Figure 3 for details. Other parameters: $n = 4$, $\lambda = 0.005$, $m_{max} = 0.5$, $N_0 = 10^4$.

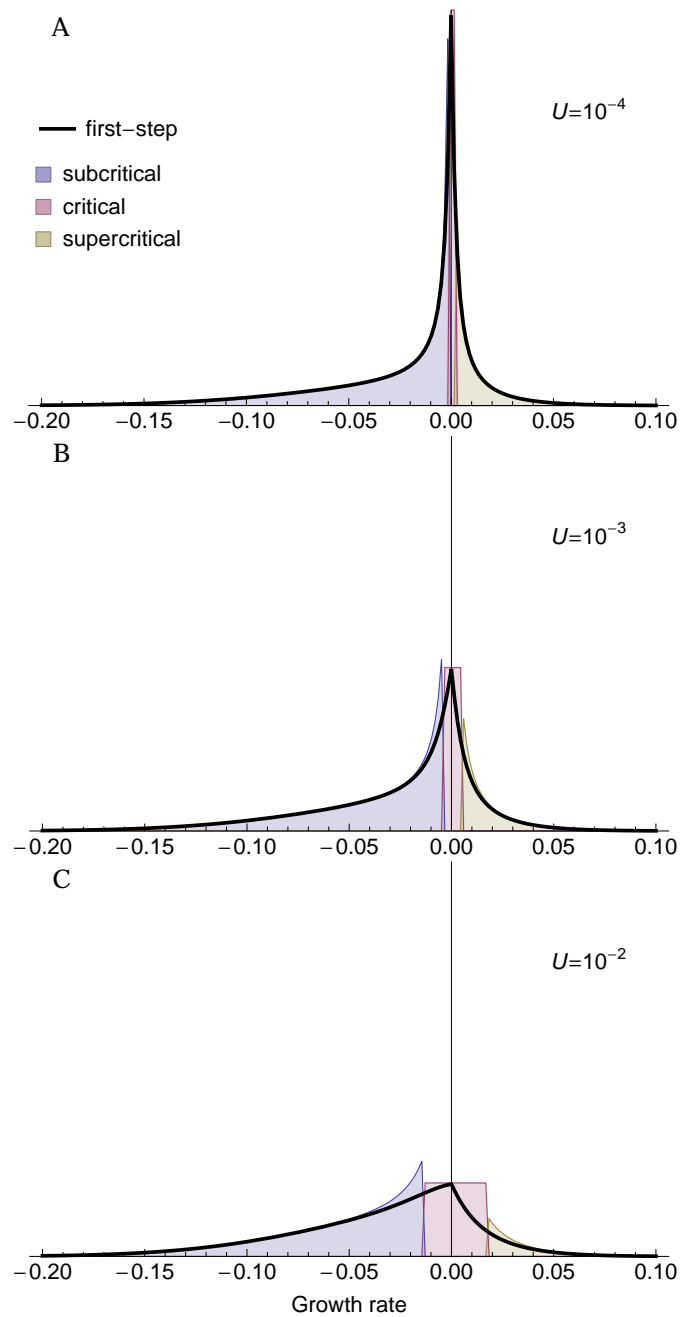


Figure S2 The distribution of first-step mutant growth rates given 2-step rescue under three mutation rates. See Figure 7 for details. Parameters: $n = 4$, $\lambda = 0.005$, $m_{max} = 0.5$, $m_0 = -0.2$.

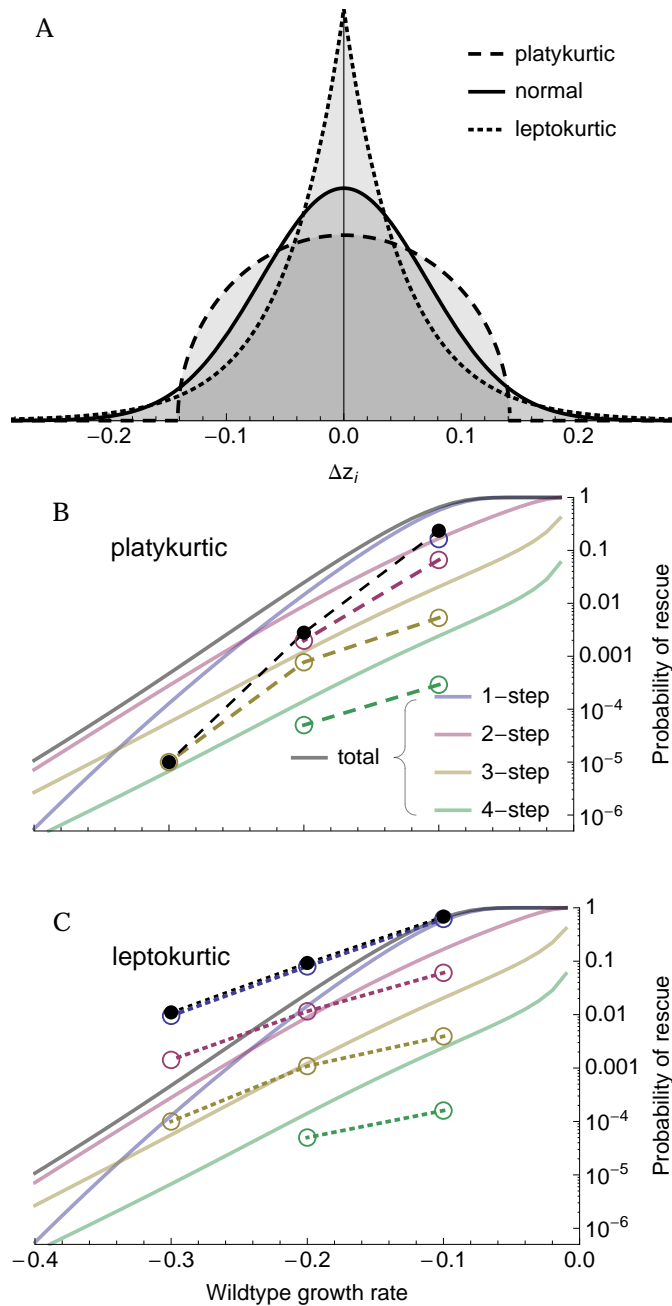


Figure S3 (A) One-dimensional slices of multidimensional platykurtic (dashed; semicircle), normal (solid; as used in main text), and leptokurtic (dotted; Laplace) mutational distributions with the same (co)variance but varying kurtosis. (B,C) The probability of 1-, 2-, 3-, or 4-step rescue with platykurtic and leptokurtic mutational distributions, respectively. The dots and broken lines represent simulation results (10^5 replicates for each wildtype growth rate). The solid lines are the numerical results for the normal mutational distribution (as in Figure 3). Parameters: $N_0 = 10^4$, $U = 2 \times 10^{-3}$, $n = 4$, $\lambda = 0.005$, $m_{max} = 0.5$.

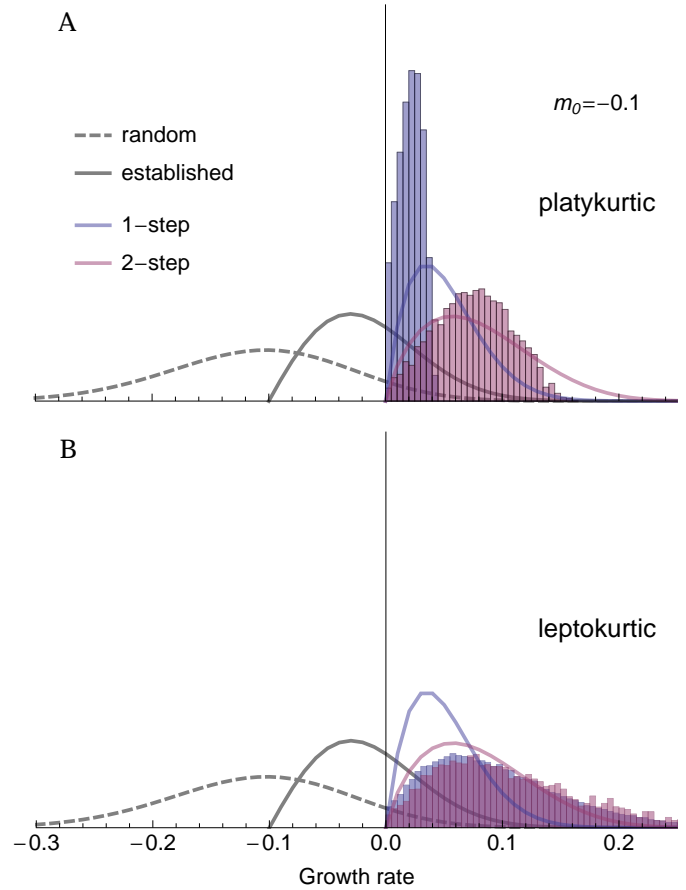


Figure S4 The distribution of growth rates among rescue genotypes under 1-step (blue) and 2-step (red) rescue with (A) platykurtic and (B) leptokurtic mutational distributions (see Figure S3A). The solid lines are predictions for a normal mutational distribution (as in Figure 6). The histograms show the distribution of growth rates among rescue genotypes observed across 10^5 replicate simulations. Parameters: $N_0 = 10^4$, $U = 2 \times 10^{-3}$, $n = 4$, $\lambda = 0.005$, $m_{max} = 0.5$, $m_0 = -0.1$.

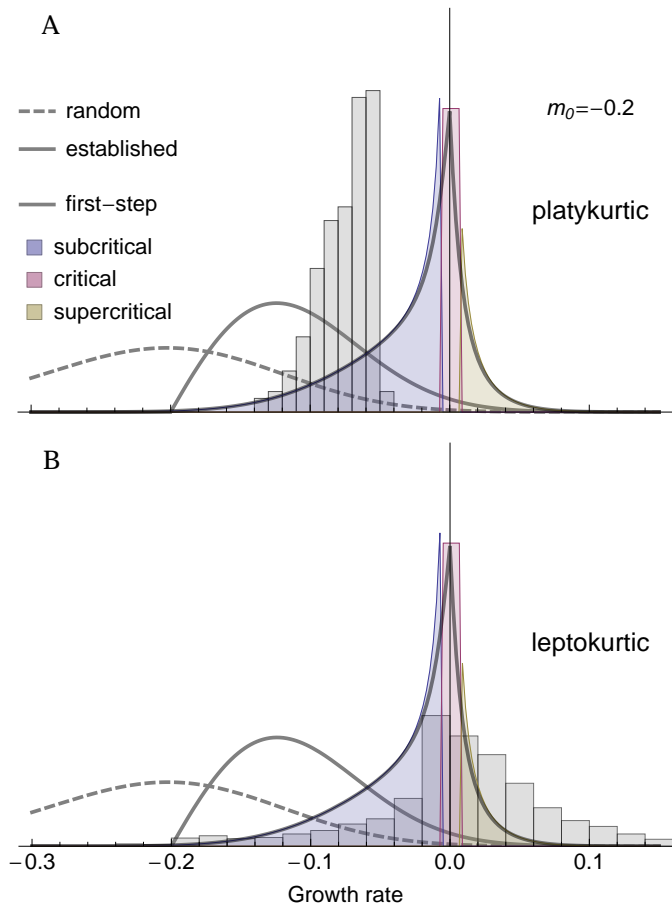


Figure S5 The distribution of growth rates among first-step mutations that lead to 2-step rescue with (A) platykurtic and (B) leptokurtic mutational distributions (see Figure S3A). The curves and shadings are predictions for a normal mutational distribution (as in Figure 7). The histograms show the distribution of growth rates observed across 10^5 replicate simulations. Parameters: $N_0 = 10^4$, $U = 2 \times 10^{-3}$, $n = 4$, $\lambda = 0.005$, $m_{max} = 0.5$, $m_0 = -0.2$.

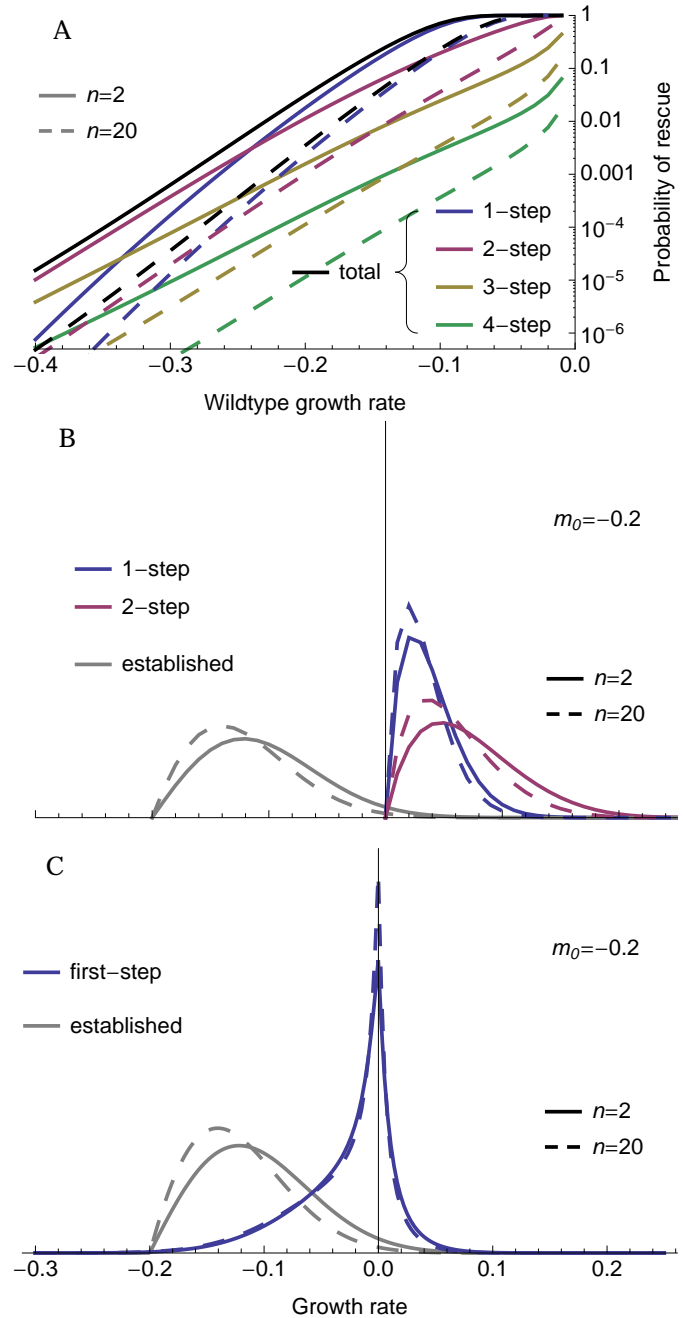


Figure S6 The effect of the number of phenotypic dimensions, n , on (A) the probability of k -step rescue, (B) the distribution of growth rates among rescue genotypes, and (C) the distribution of growth rates among first-step mutants that lead to 2-step rescue. Curves are numerical results, as in Figures 3, 6, and 7. Parameters: $N_0 = 10^4$, $U = 2 \times 10^{-3}$, $\lambda = 0.005$, $m_{max} = 0.5$.